

Depletion of CD4⁺ CD25⁺ regulatory T cells confers susceptibility to experimental autoimmune encephalomyelitis (EAE) in GM-CSF-deficient *Csf2*^{-/-} mice

Debjani Ghosh,* Alan D. Curtis II,* Daniel S. Wilkinson,* and Mark D. Mannie*,^{†,1}

*Department of Microbiology and Immunology and [†]The Harriet and John Wooten Laboratory for Alzheimer's and Neurodegenerative Disease Research, Brody School of Medicine, East Carolina University, Greenville, North Carolina, USA

RECEIVED AUGUST 13, 2015; REVISED APRIL 5, 2016; ACCEPTED MAY 4, 2016. DOI: 10.1189/jlb.3A0815-359R

ABSTRACT

Previous studies established that GM-CSF-deficient (*Csf2*-deficient) mice exhibit profound resistance to experimental autoimmune encephalomyelitis. This study addressed whether the resistance of *Csf2*-deficient mice was a result of a requirement for GM-CSF in controlling the functional balance between effector and regulatory T cell subsets during experimental autoimmune encephalomyelitis. The main observation was that treatment with the anti-CD25 mAb PC61 rendered *Csf2*-deficient mice fully susceptible to severe, chronic experimental autoimmune encephalomyelitis, with disease incidences and severities equivalent to that of C57BL/6 mice. When both donors and recipients were treated with PC61 in a passive model of experimental autoimmune encephalomyelitis, adoptive transfer of myelin-specific *Csf2*-deficient T cells into *Csf2*-deficient recipients resulted in a nonresolving chronic course of severe paralytic experimental autoimmune encephalomyelitis. The peripheral *Csf2*-deficient T cell repertoire was marked by elevated CD3⁺ T cell frequencies that reflected substantial accumulations of naïve CD44^{null-low} CD4⁺ and CD8⁺ T cells but essentially normal frequencies of CD4⁺ CD25⁺ forkhead box P3⁺ T cells among the CD3⁺ T cell pool. These findings suggested that *Csf2*-deficient mice had secondary deficiencies in peripheral T cell sensitization to environmental antigens. In accordance, myelin oligodendrocyte glycoprotein 35–55/CFA-sensitized *Csf2*-deficient mice exhibited deficient peripheral sensitization to myelin oligodendrocyte glycoprotein, whereas pretreatment of *Csf2*-deficient mice with PC61 enabled the robust induction of myelin oligodendrocyte glycoprotein-specific T cell responses in the draining lymphatics. In conclusion, the experimental autoimmune encephalomyelitis resistance of

Csf2-deficient mice, at least in part, reflects a deficient induction of effector T cell function that cannot surmount normal regulatory T cell barriers. Experimental autoimmune encephalomyelitis effector responses, however, are unleashed upon depletion of regulatory CD25⁺ T cells. *J. Leukoc. Biol.* 100: 747–760; 2016.

Introduction

EAE is widely studied as a model to resolve mechanisms underlying the pathogenesis of multiple sclerosis [1–5]. The study of EAE has revealed several molecules that have crucial roles in pathogenesis. For example, genetic deficiencies in GM-CSF [6], IL-6 [7, 8], the IL-23/IL-23R pathway [9], Stat3 [10], or Stat4 [11] confer profound resistance to disease. GM-CSF has attracted substantial attention as a result of the potential for antibody-mediated clinical intervention [12, 13]. The lack of GM-CSF in *Csf2*^{-/-} mice was associated with the lack of a sustained perivascular infiltration of the CNS during chronic EAE [6, 14]. Overall, GM-CSF was critical for the continued invasion and proliferation of leukocytes in the CNS and ultimately, for the persistence and penetration of inflammatory demyelinating lesions. Administration of exogenous GM-CSF restored EAE susceptibility in *Csf2*^{-/-} mice [6], and administration of a neutralizing anti-GM-CSF mAb inhibited disease in EAE-susceptible mice [6, 14–16]. The action of the anti-GM-CSF mAb was transient, as mice relapsed and exhibited severe EAE, ~10 d after cessation of anti-GM-CSF treatment [6, 14]. Active immunization of donor *Csf2*^{-/-} mice elicited neuroantigen-specific T cells that secreted IFN-γ and IL-17, but these T cells did not mediate the adoptive transfer of EAE [14, 16]. Conversely, adoptive transfer of GM-CSF sufficient effector T cells that were deficient in both IFN-γ and IL-17 caused severe EAE commensurate with WT T cells. Upon entry into the CNS, neuroantigen-specific T cells are known to undergo reactivation when exposed to endogenous myelin antigens on myeloid APCs [17, 18]. These

Abbreviations: CD25 = IL-2Rα, *Csf2*^{-/-} = GM-CSF deficient, DC = dendritic cell, EAE = experimental autoimmune encephalomyelitis, FIG = forkhead box p3-internal ribosome entry site-GFP knock-in, FOXP3⁺ = forkhead box P3⁺, FSC = forward-scatter, i.p. = intraperitoneal, MBP = myelin basic protein, MFI = mean fluorescence intensity, MOG = myelin oligodendrocyte glycoprotein, Ptx = pertussis toxin, T_{conv} = conventional T cell, T_{reg} = regulatory T cell, WT = wild-type

1. Correspondence: Dept. of Microbiology and Immunology, Brody School of Medicine, East Carolina University, 600 Moye Blvd., Greenville, NC 27834, USA. E-mail: mannied@ecu.edu

reactivated effector T cells secrete GM-CSF that, in turn, promotes recruitment, activation, and phagocytic activity of myeloid-derived macrophages, DCs, and microglia to facilitate EAE pathogenesis [9, 14–16, 19–21].

Based on these observations, GM-CSF is widely considered to be the signature cytokine of pathogenic effector T cells in EAE. GM-CSF is believed to be one of the few cytokines critical for EAE and is thought to mediate essential, nonredundant functions in the effector phase of EAE. Evidence presented in this study, however, reveals a more complex role of GM-CSF in homeostasis and autoimmune disease. In an active model of EAE, pretreatment of MOG35–55/CFA-sensitized *Csf2*^{−/−} mice with the anti-CD25 PC61 mAb caused the depletion of CD4⁺ CD25⁺ FOXP3⁺ T cells and unleashed an encephalitogenic immune response that culminated in a chronic course of severe paralytic EAE. In a passive model of EAE, pretreatment of MOG35–55/CFA-sensitized *Csf2*^{−/−} donors with the PC61 mAb enabled the generation of pathogenic T cells that transferred severe paralytic EAE to *Csf2*^{−/−} recipients. Additional treatment of *Csf2*^{−/−} recipients with the anti-CD25 mAb enabled chronic nonresolving EAE in those recipients. The induction of severe paralytic EAE in *Csf2*^{−/−} mice reveals that GM-CSF, at least in part, controls disease susceptibility in EAE by setting the functional balance of effector and T_{reg} subsets.

MATERIALS AND METHODS

Animals and reagents

C57BL/6, FIG (B6.Cg-*Foxp3*^{tm2Tch}/J; Stock Number 006772), and 2D2 [C57BL/6-Tg(Tcra2D2, Tcrb2D2, 1Kuch/J); Stock No. 006912] strains were obtained from The Jackson Laboratory (Bar Harbor, ME, USA) and were housed and bred in the Department of Comparative Medicine at East Carolina University (Greenville, NC, USA). The GM-CSF-deficient B6.*Csf2*^{−/−} strain was a generous gift from Dr. Glenn Dranoff [22]. This strain lacked the ability to synthesize GM-CSF and was resistant to EAE. FIG *Csf2*^{−/−} and 2D2-FIG *Csf2*^{−/−} strains were obtained by standard breeding techniques. *Csf2*^{−/−} and FIG *Csf2*^{−/−} mice were genotyped by PCR amplification of tail-snip DNA. The FIG genotype was determined by use of forward (5′-CAC CTA TGC CAC CCT TAT CC-3′) and reverse (5′-ATT GTG GGT CAA GGG GAA G-3′) primers. The FIG knock-in product was 390 bp, and the WT product was 341 bp. B6.*Csf2*^{−/−} genotyping was performed via a neomycin-specific primer (5′-AGG CCA CTT GTG TAG CGC CAA GT-3′), a *Csf2* common exon 2-specific primer (5′-TCG TCT CTA ACG AGT TCT CCT TCA-3′), and WT exon 3-specific primer (5′-TGC TCG AAT ATC TTC AGG-3′). The expected *Csf2*^{−/−} mutant WT targets were 600 and 800 bp, respectively. Animal care and use were performed in accordance with approved animal use protocols and guidelines of the East Carolina University Institutional Animal Care and Use Committee (Animal Use Protocols K147b, 156, and 158). 2D2 mice have a MOG-specific, self-reactive T cell repertoire. Routine screening of 2D2 mice was performed by FACS analysis of PBMC by use of antibodies specific for TCR Vβ11 and/or Vα3.2. Synthetic peptide MOG35–55 was comprised of the following sequence: M-E-V-G-W-Y-R-S-P-F-S-R-V-V-H-L-Y-R-N-G-K.

Flow cytometric analyses of PBMC

Splenocytes were processed to a single-cell suspension and washed 3 times in HBSS. PBMCs were collected via the submandibular vein in 130 mM sodium citrate buffer and washed in HBSS with 2% heat-inactivated FBS. Cells were then stained for 1 h at 4°C in the dark with designated cocktails of fluorochrome-conjugated antibodies, including those specific for CD45 (30-F11), CD3 (17A2), CD4 (GK1.5), CD8, (53–6.7), CD19 (6D5), Ly6G (1A8), CD44 (IM7), and I-A^b (AF6-120.1). After staining PBMC, erythrocytes were

lysed with 1:10 HBSS for 20 s, followed by addition of 2× PBS. Data were collected by use of a BD LSRII flow cytometer (BD Biosciences, Franklin Lakes, NJ, USA) and analyzed by use of FlowJo software. Bar graphs show the mean, and error bars show the SEM, unless designated otherwise. Pairwise comparisons between *Csf2*^{−/−} and WT samples were analyzed by 2-tailed *t* tests for data that passed normality (Shapiro-Wilk) and equal variance (Brown-Forsythe) tests. Otherwise, data were assessed with a Mann-Whitney rank sum test. In designated experiments, reference "counting" beads were added to samples immediately before flow cytometric analysis (AccuCheck counting beads; Thermo Fisher Scientific, Waltham, MA, USA). The use of reference beads enabled comparisons of cell yield or absolute cell numbers.

Generation, purification, and administration of the mAb

The PC61-5.3 anti-CD25 rat IgG1(λ), Y13-259 anti-v-H-Ras rat IgG1(κ), R4-6A2 anti-IFN-γ rat IgG1(κ), GK1.5 anti-CD4 rat IgG2b(κ), and 53-6.7 anti-CD8 rat IgG2a(κ) hybridomas were used as a source of depleting antibodies or control mAb. Initial preparations of PC61 mAb (anti-CD25 mAb) and Y13-259 mAb (rat IgG1 isotype control) were generous gifts from Dr. Gregory Sempowski (Duke University School of Medicine, Durham, NC, USA). Subsequent PC61 and Y13 mAb preparations were expressed and purified at East Carolina University. The PC61-5.3 and Y13-259 hybridomas were obtained from American Type Culture Collection (Manassas, VA, USA) and were subcloned twice to ensure stability. For all 5 hybridomas, cells were cultured in supplemented DMEM in C2011 hollow fiber cartridges (FiberCell Systems, Frederick, MD, USA). Hybridoma supernatants were clarified at 7200 g, precipitated with 50% ammonium sulfate, and dissolved in PBS. mAb preparations were purified on protein G agarose columns. Antibody was eluted with 200 mM glycine at pH 3.0 and immediately neutralized by 1 M Tris buffer of pH 9.0. IgG fractions were also purified by ultrafiltration on YM100 membranes in Amicon-stirred cell cylinders. The purity of these mAb was verified by SDS-PAGE. Specific activities of all PC61 preparations were determined by staining of murine CD25⁺ T cells with serial 1/2-log dilutions of the mAb. After washing, PC61-stained T cells were labeled with a PE-conjugated goat anti-rat IgG(H+L) secondary antibody, followed by flow cytometric analysis. As designated for pretreatment experiments, purified mAb were administered at a dose of 250 μg/injection i.p. to mice on d −5 and −3 (or d −4 and −2) unless designated otherwise. Depletion of specific lymphoid subsets was confirmed by flow cytometric analysis of PBMC on d −1 or 0. Active immunization with MOG35–55 in CFA was initiated on d 0.

Induction and assessment of EAE

For active induction of EAE, CFA [4 mg/ml heat-killed *Mycobacterium tuberculosis* H37Ra (BD Biosciences) in IFA] was mixed 1:1 with MOG35–55 in saline and emulsified by sonication. A total dose of 200 μg MOG35–55/CFA was injected across the lower back via 3 spaced subcutaneous injections (~0.033 ml/injection) for a total injection volume of 0.1 ml/mouse. Mice also received injections of 200 ng i.p. Ptx (List Biological Laboratories, Campbell, CA, USA) on d 0 and 2. All immunizations were given under isoflurane anesthesia (Abbott Laboratories, Chicago, IL, USA). For passive induction of EAE, draining lymph nodes and spleen were pooled from donor MOG/CFA-immunized mice and were cultured with 1 μM MOG35–55 and 10 ng/ml IL-23 for 3 d. Cultured T cells were washed extensively in HBSS, and 10⁷ cells were injected i.p. into each recipient. Recipients were given 200 ng i.p. Ptx on d 1 and 3. Mice were assessed daily for clinical score and body weight. The following scale was used to score EAE: 0, no disease; 0.5, partial paralysis of tail without ataxia; 1.0, flaccid paralysis of tail or ataxia but not both; 2.0, flaccid paralysis of tail with ataxia or impaired righting reflex; 3.0, partial hindlimb paralysis marked by inability to walk upright but with ambulatory rhythm in both legs; 3.5, same as above but with full paralysis of 1 leg; 4.0, full hindlimb paralysis of both legs; 5.0, total hindlimb paralysis with forelimb involvement or moribund. A score of 5.0 was a humane endpoint for euthanasia.

Cumulative EAE scores were calculated by summing daily scores for each mouse. Maximal scores were calculated as the most severe EAE score for each mouse. Mice that did not exhibit EAE had a score of 0 for the cumulative and

maximal scores, and these scores were included in the group average. To calculate percent maximal weight loss, 100% body weight was assigned as the maximal body weight obtained from d 1 through d 10, and daily body weights were calculated for each day after normalization to this 100% value. The minimum body weight was defined as the lowest body weight during the entire course of EAE after normalization to the 100% value. Maximal weight loss was calculated by subtraction of the normalized minimum value from the maximum 100% value. Average daily weight loss was calculated as the average of daily body-weight measurements from d 10 until the end of experiment, subtracted from the 100% maximal body weight. Cumulative and maximal EAE scores were converted to ranked scores and analyzed by nonparametric ANOVA. Weight loss was analyzed by parametric ANOVA. Nonparametric and parametric ANOVA were assessed with a Bonferroni post hoc test. Error bars portraying data for EAE clinical scores and weight loss represent the SEM. After humane euthanasia, the spinal column and brain were removed and were fixed in 10% neutral-buffered formalin. Sections were prepared from the spinal cord, brain, brainstem, and cerebellum. Sections were stained with H&E and were imaged with a Leica DFC420C digital camera connected to a Leica DM400B microscope.

RESULTS

Depletion of the CD4⁺CD25⁺ T cell subset in *Csf2*^{-/-} mice restored susceptibility to EAE

Experiments were performed to assess whether a T_{reg} pathway may contribute to the EAE resistance of *Csf2*^{-/-} mice. In preliminary experiments, treatment of C57BL/6 mice with the PC61 anti-CD25 mAb purged CD4⁺ CD25⁺ T_{regs} from the blood and spleen for >20 d, followed by a rebound to normal levels by d 40, whereas the Y13 mAb (anti-p21 v-H-Ras rat IgG1 isotype control) had no effect on CD25⁺ T cell levels (data not shown). Experiments were then performed to assess whether a pre-dominant T_{reg} pathway may contribute to the EAE resistance of *Csf2*^{-/-} mice (Fig. 1A–D and Table 1). *Csf2*^{-/-} or C57BL/6 mice were pretreated with 250 µg purified anti-CD25 PC61 mAb on d -4 and -2 to clear the CD4⁺ CD25⁺ T cell subset. Mice were immunized with 200 µg MOG35–55 in CFA on d 0 and injected with Ptx (200 ng) i.p. on d 0 and 2, according to the standard EAE induction protocol. In the first experiment, PC61 pretreatment of *Csf2*^{-/-} mice abrogated the EAE resistance of this strain. However, PC61 had no significant impact on EAE in C57BL/6 mice (Experiment 1 of Fig. 1A and Table 1), most likely because the 200 µg dosage of MOG35–55 overwhelmed any T_{reg} resistance. PC61-pretreated *Csf2*^{-/-} mice differed qualitatively from control *Csf2*^{-/-} mice in the mean cumulative score (52.7 vs. 0.0) and mean maximal score (3.0 vs. 0.0), respectively (Table 1). As PC61 did not affect EAE in WT mice, 2 replicate experiments were performed to compare the EAE susceptibility of PC61 pretreated *Csf2*^{-/-} mice, control *Csf2*^{-/-} mice, and WT C57BL/6 mice. In both replicate experiments, PC61 pretreatment abrogated the EAE resistance of *Csf2*^{-/-} mice and enabled severe paralytic disease (Table 1, Experiments 2 and 3). Statistical analysis of the compiled data showed that PC61 pretreatment profoundly affected EAE in *Csf2*^{-/-} mice, as measured by EAE incidence and both mean cumulative and mean maximal scores (Table 1). Clinical signs of EAE in *Csf2*^{-/-} mice reflected classic rather than atypical disease manifestations.

The individual maximal scores for each mouse for the 3 combined experiments are shown in Fig. 1B (legend applies to Fig. 1, B–D and G–I). One-half of the PC61-pretreated *Csf2*^{-/-}

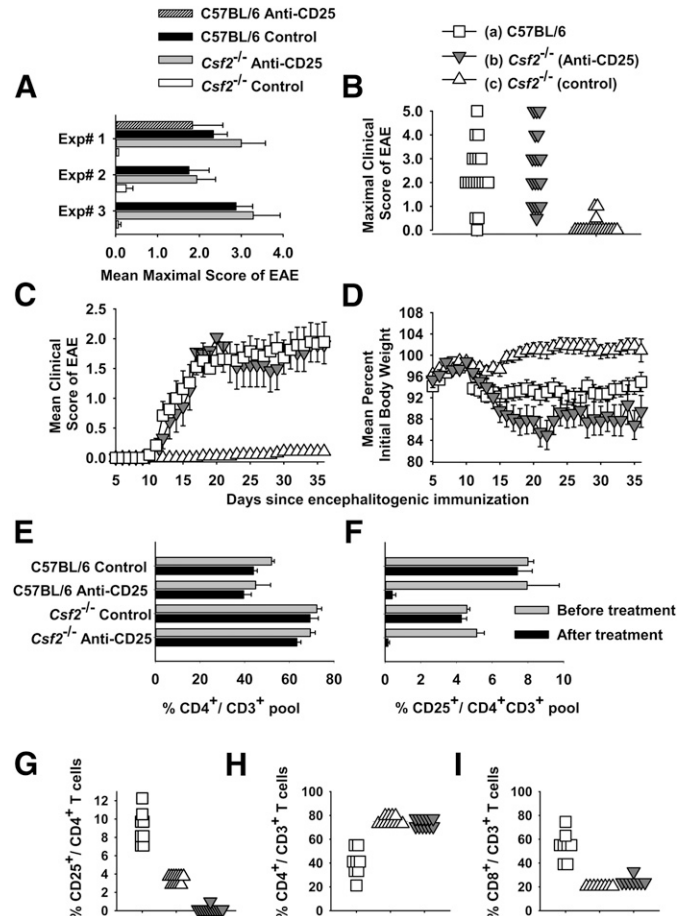


Figure 1. The PC61 anti-CD25 mAb enables the active induction of EAE in *Csf2*^{-/-} mice. (A–I) C57BL/6 or *Csf2*^{-/-} mice were or were not pretreated with 250 µg purified PC61 mAb on d -4 and -2 i.p. (A–D) Shown are individual (A) or pooled (B–D) data from Experiments 1–3 of Table 1. Mice were immunized with 200 µg MOG35–55 in CFA subcutaneously on d 0 and injected with Ptx (200 ng) i.p. on days 0 and 2. (A) Mean maximal scores (±SEM) are shown for Experiments 1–3 (*Csf2*^{-/-} with and without PC61, $P < 0.02$ for all 3 experiments). (B) Frequency analysis of the mean maximal scores are shown for data pooled from Experiments 1–3 for WT mice ($n = 19$), *Csf2*^{-/-} mice treated with PC61 ($n = 18$), and *Csf2*^{-/-} control mice [$n = 19$; (c) vs. (b) and (a), $P < 0.001$]. This description also applies to C and D and G–I. (C and D) The daily mean maximal scores and weight loss are shown for data pooled from Experiments 1–3. Daily mean clinical scores for (a) vs. (c) (d 12 and 13, $P < 0.005$; d 14–36, $P < 0.001$) and (b) vs. (c) (d 15 and 16, $P < 0.05$; d 17–36, $P < 0.001$) were assessed by nonparametric ANOVA. Daily body weight values for (a) vs. (c) (d 11–13 and d 16–36, $P < 0.05$) and (b) vs. (c) (d 15, $P = 0.008$; d 16–36, $P < 0.005$) were assessed by parametric ANOVA. (E and F) C57BL/6-PC61 and *Csf2*^{-/-}-PC61 groups on d -4 before treatment vs. d 0 after treatment ($n = 3$, $P < 0.01$). (G) All comparisons, $P < 0.001$. (H and I) (a) vs. (b) and (c), $P < 0.001$.

mice had severe EAE scores (≥ 3.0), commensurate with that of control WT mice. In Experiment 3, 3 of 7 *Csf2*^{-/-} mice in the anti-CD25 pretreatment group reached a humane endpoint (score of 5.0) on d 21, 22, and 28 and were thereafter excluded from scoring. The time course for mean maximal EAE in

TABLE 1. Pretreatment of *Csf2*^{-/-} mice with the anti-CD25 PC61 mAb enabled severe paralytic EAE

Experiment number	Strain	Treatment	Incidence	Mean cumulative score	Median cumulative score	Mean maximal score	Median maximal score
1	C57BL/6	Anti-CD25	3 of 3	39.3 ± 21.0	45.0	1.8 ± 0.7	2.0
	C57BL/6	Saline	3 of 3	34.0 ± 11.9	25.5	2.3 ± 0.3	2.0
	<i>Csf2</i> ^{-/-}	Anti-CD25	3 of 3	52.7 ± 25.7	57.5	3.0 ± 0.6	3.0
	<i>Csf2</i> ^{-/-}	Saline	0 of 3	0.0 ± 0.0	0.0	0.0 ± 0.0	0.0
2	C57BL/6	Saline	7 of 8	19.3 ± 6.6	16.8	1.8 ± 0.5	2.0
	<i>Csf2</i> ^{-/-}	Anti-CD25	8 of 8	29.4 ± 9.3	17.5	1.9 ± 0.4	1.5
	<i>Csf2</i> ^{-/-}	Saline	2 of 8	2.1 ± 1.6	0.0	0.3 ± 0.2	0.0
	C57BL/6	Saline	8 of 8	63.3 ± 8.9	51.3	2.9 ± 0.4	2.5
3	<i>Csf2</i> ^{-/-}	Anti-CD25	7 of 7	32.5 ± 7.2	37.0	3.3 ± 0.6	3.0
	<i>Csf2</i> ^{-/-}	Saline	1 of 8	0.9 ± 0.9	0.0	0.1 ± 0.1	0.0
	(a) C57BL/6	Saline	18 of 19	46.8 ± 8.6	51.0	2.3 ± 0.3	2.0
	(b) <i>Csf2</i> ^{-/-}	Anti-CD25	18 of 18	37.2 ± 6.3	31.5	2.6 ± 0.4	2.5
1–3	(c) <i>Csf2</i> ^{-/-}	Saline	3 of 19	1.4 ± 0.8	0.0	0.1 ± 0.1	0.0
1–3	(c) vs. (a) and (b)		<i>P</i> < 0.0001	<i>P</i> < 0.001		<i>P</i> < 0.001	

These data are portrayed in Fig. 1. C57BL/6 or *Csf2*^{-/-} mice were or were not pretreated with 250 μg purified PC61 mAb on d -4 and -2 i.p. Mice were immunized with 200 μg MOG35–55 in CFA on d 0 and injected with Ptx (200 ng) i.p. on d 0 and 2. Shown are the mean/median cumulative and maximal scores (±SEM) for 3 independent experiments scored through d 36. Differences in cumulative and maximal EAE scores were assessed by nonparametric ANOVA. Differences in disease incidence were assessed pairwise by a Fisher's exact test.

PC61-pretreated *Csf2*^{-/-} mice and control WT mice was essentially identical (Fig. 1C; data pooled for Groups a, b, and c from Experiments 1, 2, and 3). Maximal and average weight loss in PC61-treated *Csf2*^{-/-} mice (18.9% ± 2.6 and 11.0% ± 2.0) also differed significantly from *Csf2*^{-/-} control mice (7.2% ± 1.4 and -0.4% ± 1.2; parametric ANOVA, *P* < 0.001, *P* < 0.001), respectively. These differences are portrayed as a time course in Fig. 1D. The time course for mean body weight showed that the body weight of PC61-pretreated *Csf2*^{-/-} mice trended below that of WT mice (Fig. 1D). In contrast, control *Csf2*^{-/-} mice did not exhibit severe EAE and had stable body weights during the entire disease course. Overall, these data indicated that the CD4⁺ CD25⁺ T_{reg} subset constituted a major barrier to the induction of EAE in GM-CSF-deficient mice.

For mice shown in Fig. 1A, assessments taken on d -4 (before initiation of treatment with PC61) and d 0 (after treatment) showed only a modest decrease of the global CD4⁺ pool (Fig. 1E) but a complete PC61-dependent loss of CD25⁺ CD4⁺ T cells in the CD4⁺ T cell pool (Fig. 1F). Unexpectedly, these data also revealed that *Csf2*^{-/-} mice had higher percentages of CD4⁺ T cells in the CD3⁺ T cell pool (Fig. 1E) and lower percentages of CD4⁺ CD25⁺ T cells in the CD4⁺ pool compared with C57BL/6 mice (Fig. 1F), and these strain-dependent differences were independent of PC61 mAb treatment. Experiments with larger cohorts of mice showed that pretreatment with PC61 eliminated CD4⁺CD25⁺ T cells from PBMC without affecting circulating levels of CD4⁺ or CD8⁺ T cells (Fig. 1G–I). The loss of CD25⁺ cells from PBMC was a result of cell depletion rather than CD25 down-modulation, as assessed by staining of PBMC with a PE-conjugated anti-rat IgG(H+L) reagent (data not shown). Overall, these data confirmed PC61-mediated elimination of CD25⁺ T cells and also revealed significant perturbations of T cell subsets in PBMC of *Csf2*^{-/-} mice.

PC61-pretreated *Csf2*^{-/-} mice that showed severe paralytic EAE (Fig. 1) also had extensive perivascular and periventricular inflammatory lesions in the CNS (Fig. 2). Inflammatory lesions

were noted in the cerebellum (Fig. 2A and D), hindbrain (Fig. 2B and E), brainstem (Fig. 2C and F), and spinal cord (Fig. 2G–J). Both periventricular and perivascular lesions were noted throughout in midbrain and hindbrain. In addition to brain

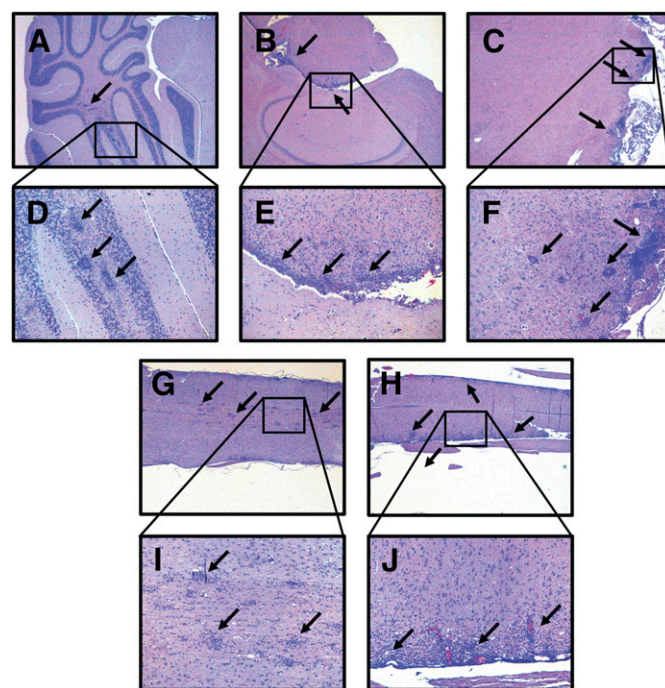


Figure 2. GM-CSF-deficient *Csf2*^{-/-} mice pretreated with PC61 exhibited extensive perivascular and periventricular CNS lesions. Portrayed are representative sections of *Csf2*^{-/-} mice afflicted with severe paralytic EAE (Fig. 1), including the cerebellum (A and D), hindbrain (B and E), brainstem (C and F), and spinal cord (G and I and H and J). Mononuclear inflammatory lesions are marked by black arrows. Images were acquired at 25× original magnification (A–C, G, and H) or 100× original magnification (D–F, I, and J).

involvement, EAE in *Csf2*^{-/-} mice was associated with numerous focal lesions together with extensive periventricular infiltration in the spinal cord. The images portray 3 representative *Csf2*^{-/-} mice with full hindlimb paralysis (clinical score = 4.0). Thus, active induction of EAE in PC61-pretreated *Csf2*^{-/-} mice elicited both clinical and histologic signs of severe EAE.

The PC61 mAb was tested side by side with the anti-IFN- γ mAb R4.6A2 as a specificity control in *Csf2*^{-/-} mice (Fig. 3A and B and Table 2). Conceptually, both PC61 and anti-IFN- γ mAb should augment disease [23–27], although the R4.6A2 mAb should have a minimal impact on EAE based on the paradigm used in Fig. 3, as R4.6A2 would need continuous application

throughout the time course to have an effect. Both R4.6A2 and PC61 mAb were rat IgG1 mAb. These mAb were injected on d -4 and -2 (250 μ g/dose), followed by active immunization on d 0 with MOG35–55/CFA with injections of Ptx on d 0 and 2. Mice were assessed for EAE and body weight for 41 continuous days. PC61-pretreated mice differed significantly from R4.6A2 mAb or saline-pretreated mice in the mean scores for cumulative disease (77.3 \pm 10.0 vs. 8.6 \pm 3.0 or 4.3 \pm 4.3, P < 0.001), maximal disease (3.6 \pm 0.3 vs. 1.0 \pm 0.3 or 0.3 \pm 3, P \leq 0.001), and maximal weight loss (29.3 \pm 2.0% vs. 7.8 \pm 2.9% or 4.0 \pm 3.0%, P < 0.001), respectively. The time courses of EAE and weight loss are shown in Fig. 3A and B. The daily mean clinical scores for

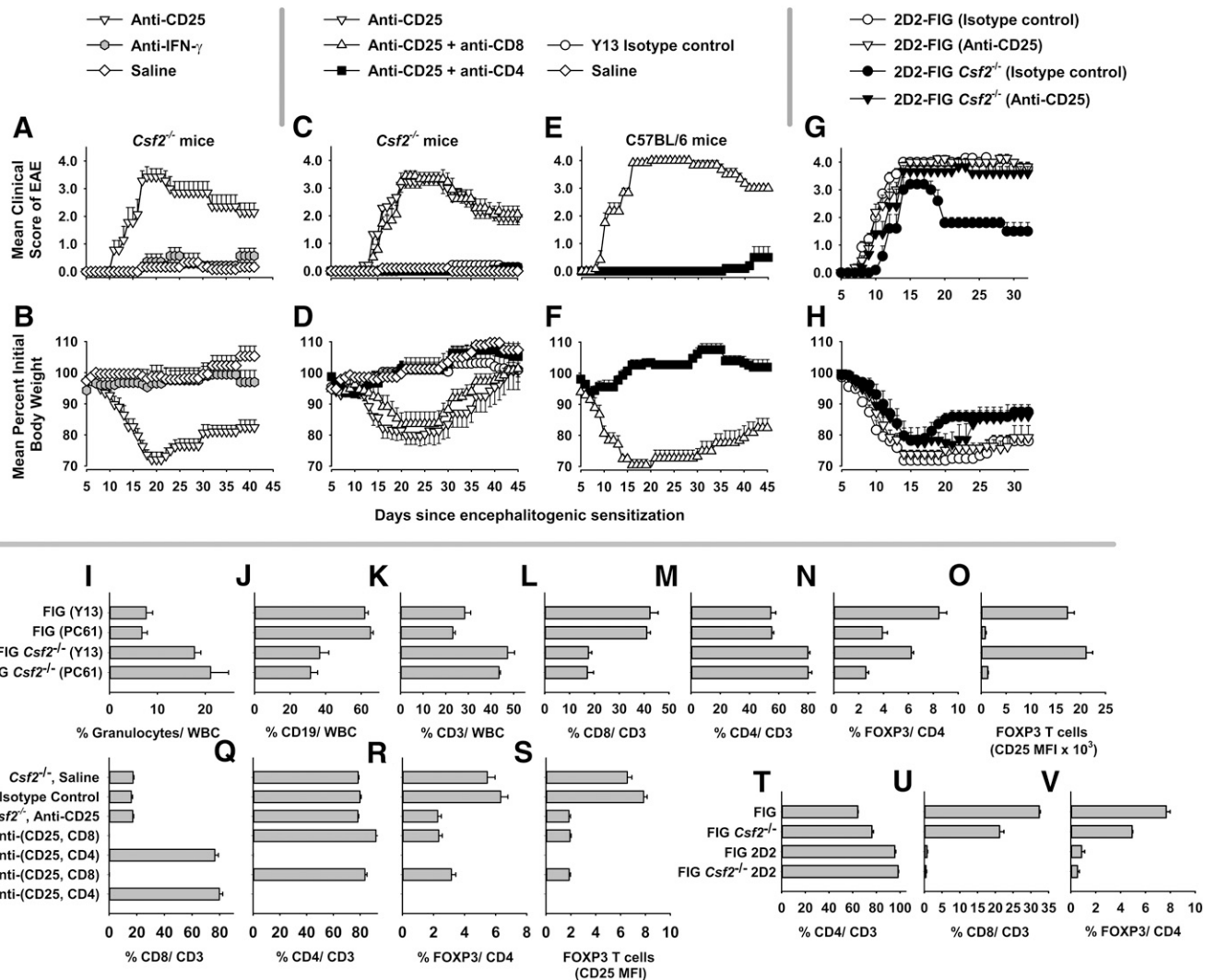


Figure 3. Depletion of CD25⁺ T_{regs} enables CD4⁺ T cell-mediated EAE in the resistant *Csf2*^{-/-} strain. (A–H) Shown are EAE and weight-loss time courses for data portrayed in Table 2 (A–F) and Table 3 (G and H). Designated mouse strains were injected i.p. with purified R4.6A2 anti-IFN- γ rat IgG1, PC61 anti-CD25 rat IgG1, Y13 isotype control rat IgG1, GK1.5 anti-CD4 rat IgG2b, and/or 53.6-7 anti-CD8a rat IgG2a on d -5 and -3 (or d -4 and -2). All mAb were injected at a dose of 250 μ g/mAb/injection. Mice were immunized on d 0 with 200 μ g MOG35–55 in CFA with i.p. injections of Ptx on d 0 and 2. Mice were scored and weighed daily. (I–O) FIG and FIG *Csf2*^{-/-} mice (n = 4) were injected with PC61 or Y13 mAb on d -4 and -2, and then PBMCs were analyzed for expression of CD45, Ly6G, CD19, CD3, CD4, CD8, FOXP3 (GFP), and CD25 on d 0. FIG vs. FIG *Csf2*^{-/-} mice (analysis of Y13 groups or PC61 groups separately). (I–M) P < 0.001, both comparisons; (O) P < 0.02, both comparisons; (N) all comparisons, P < 0.005. (O) PC61 vs. Y13, P < 0.001, both comparisons. (P–S) These data represent PBMC analyses (d 0) of mice used in C–F. In groups treated with anti-CD8 and anti-CD4 mAb, percentages were <0.2% for each CD8⁺ and CD4⁺ subset, respectively (P < 0.001 vs. all other groups). (R and S) Anti-CD25 (\pm anti-CD8) groups vs. saline or Y13 groups, P < 0.001. (T–V) Naïve, unmanipulated 2D2-FIG or 2D2-FIG *Csf2*^{-/-} vs. non-2D2 groups, P < 0.001.

TABLE 2. EAE in *Csf2*^{-/-} mice was enabled by an anti-CD25 mAb and reversed by an anti-CD4 mAb

Figure	Strain	mAb pretreatment	Incidence	Means (\pm SE) cumulative scores	<i>P</i>	Means (\pm SE) maximal scores	<i>P</i>	% Maximal weight loss	<i>P</i>
3A and B	<i>Csf2</i> ^{-/-}	No mAb	1 of 6	4.3 \pm 4.3	*	0.3 \pm 0.3	*	4.0 \pm 3.0%	*
3A and B	<i>Csf2</i> ^{-/-}	Anti-IFN- γ	7 of 8	8.6 \pm 3.0	ns	1.0 \pm 0.3	ns	7.8 \pm 2.9%	ns
3A and B	<i>Csf2</i> ^{-/-}	Anti-CD25	7 of 7	77.3 \pm 10.0	<0.001	3.6 \pm 0.3	<0.001	29.3 \pm 2.0%	<0.001
3C and D	<i>Csf2</i> ^{-/-}	No mAb	1 of 5	1.5 \pm 1.5	*	0.1 \pm 0.1	*	4.4 \pm 2.2%	*
3C and D	<i>Csf2</i> ^{-/-}	Y13 isotype control	2 of 7	3.7 \pm 2.4	ns	0.2 \pm 0.1	ns	6.1 \pm 1.7%	ns
3C and D	<i>Csf2</i> ^{-/-}	Anti-CD25	9 of 9	82.3 \pm 6.6	<0.001	3.3 \pm 0.2	<0.001	21.8 \pm 3.5%	0.008
3C and D	<i>Csf2</i> ^{-/-}	Anti-CD25 + anti-CD8	9 of 9	80.1 \pm 7.1	<0.001	3.6 \pm 0.2	<0.001	17.6 \pm 3.9%	ns
3C and D	<i>Csf2</i> ^{-/-}	Anti-CD25 + anti-CD4	1 of 8	0.6 \pm 0.6	ns	0.1 \pm 0.1	ns	7.9 \pm 2.5%	ns
3E and F	C57BL/6	Anti-CD25 + anti-CD8	6 of 6	124.8 \pm 1.9	<0.001	4.0 \pm 0.0	<0.001	32.0 \pm 2.0%	<0.001
3E and F	C57BL/6	Anti-CD25 + anti-CD4	2 of 5	2.7 \pm 1.7	ns	0.5 \pm 0.4	ns	5.7 \pm 1.9%	ns

These data are portrayed in Fig. 3A–F. (Fig. 3A and B) Designated mouse strains were injected i.p. with purified R4.6A2 anti-IFN- γ rat IgG1 or PC61 anti-CD25 rat IgG1 mAb on d -4 and -2. (Fig. 3C–F) Alternatively, mice were injected with PC61, Y13 (isotype control rat IgG1), GK1.5 (anti-CD4 rat IgG2b), and/or 53.6-7 (anti-CD8a rat IgG2a) mAb on d -5 and -3. All mAb were injected at a dose of 250 μ g/injection. Mice were immunized on d 0 with 200 μ g MOG35–55 in CFA with i.p. injections of Ptx on d 0 and 2. Mice were scored and weighed daily. Shown are the mean cumulative and maximal scores (\pm SEM). ns, not significant; asterisk indicates control group.

PC61-pretreated mice differed significantly from the scores for R4.6A2 mAb-pretreated mice on d 11–41 ($P \leq 0.02$) or saline-pretreated mice on d 13–37 ($P \leq 0.002$). The daily weight loss scores for PC61-pretreated mice significantly differed from those for R4.6A2 mAb-pretreated mice on d 14 and 15 and d 30–37 ($P \leq 0.004$), d 16–29 ($P \leq 0.0001$), and d 38–41 ($P = 0.024$). The daily weight loss scores for PC61-pretreated mice also differed significantly from those for saline-pretreated mice on d 14–29 and d 38–41 ($P \leq 0.0001$) and d 30–37 ($P \leq 0.006$). As the administration of the mAb did not span the time course of disease, no conclusions were rendered regarding the role of IFN- γ in the EAE susceptibility of *Csf2*^{-/-} mice. Rather, these data indicated that the anti-CD25 specificity of the PC61 mAb was needed to enable EAE susceptibility.

As EAE in PC61-treated *Csf2*^{-/-} mice was uncharted, we considered the possibility that alternative effector T cell subsets, including CD8⁺ effector T cells, may facilitate EAE pathogenesis in this model [28–32]. To test this possibility, PC61 was used to deplete CD25⁺ T_{regs} in conjunction with mAb-mediated depletion of either the CD4⁺ subset (GK1.5 mAb) or the CD8⁺ subset (53.6-7 mAb; Fig. 3C and D and Table 2). In these experiments, the Y13-259 mAb was used as an isotype control for

PC61. The results showed that *Csf2*^{-/-} mice treated with PC61 alone or with an anti-CD8 mAb exhibited severe, chronic EAE, whereas *Csf2*^{-/-} mice treated with PC61 and anti-CD4 mAb were resistant to EAE. As expected, the anti-CD4 mAb also inhibited EAE in C57BL/6 mice (Fig. 3E and F and Table 2). Thus, the anti-CD8 mAb had no effect on the disease course, whereas the anti-CD4 mAb abrogated EAE. These data indicated that this model of PC61-dependent EAE in *Csf2*^{-/-} mice was mediated by CD4⁺ effector T cells rather than CD8⁺ T cells. *Csf2*^{-/-} mice treated with saline or the Y13 isotype control mAb were equally resistant to EAE.

A second experiment focused on 2D2-FIG mice that were or were not bred to include the *Csf2*^{-/-} genotype (Fig. 3G and H and Table 3). 2D2-FIG mice bear the 2D2 V β 11/V α 3.2 transgenic TCR specific for I-A^b/MOG35–55 and a GFP reporter of FOXP3 expression. These mice have a deficiency of CD8⁺ T cells as a result of allelic exclusion and the positive selection of this clonotype on I-A^b in the thymus. Although these mice are *Rag1*/2 sufficient, these mice nonetheless have a relative deficiency in FOXP3⁺ T cells compared with WT mice as a result of the clonotypic homogeneity of the 2D2 repertoire. Naïve 2D2-FIG mice typically have a FOXP3⁺ repertoire ranging from 0.1 to

TABLE 3. Spontaneous recovery in transgenic 2D2 mice was facilitated by endogenous GM-CSF

Figure	Strain	mAb pretxt	Incidence	Means (\pm SE) maximal scores (overall)	<i>P</i>	Means (\pm SE) maximal scores (d 20–32)	<i>P</i>	% Maximal weight loss (d20–32)	<i>P</i>
3G and H	2D2-FIG	Y13 isotype control	7 of 7	4.3 \pm 0.2	ns	4.3 \pm 0.2	<0.001	28.8 \pm 3.4%	0.027
3G and H	2D2-FIG	Anti-CD25	8 of 8	4.3 \pm 0.2	ns	4.3 \pm 0.2	<0.001	25.5 \pm 1.8%	ns
3G and H	2D2-FIG <i>Csf2</i> ^{-/-}	Y13 isotype control	5 of 5	3.2 \pm 0.4	*	1.8 \pm 0.2	*	14.9 \pm 1.9%	*
3G and H	2D2-FIG <i>Csf2</i> ^{-/-}	Anti-CD25	6 of 6	3.8 \pm 0.3	ns	3.8 \pm 0.3	=0.008	24.4 \pm 4.2%	ns

These data are portrayed in Fig. 3G and H. 2D2-FIG and 2D2-FIG *Csf2*^{-/-} mice were injected with PC61 or Y13 (isotype control) on d -4 and -2. All mAb were injected at a dose of 250 μ g/mAb/injection. Mice were immunized on d 0 with 200 μ g MOG35–55 in CFA with i.p. injections of Ptx on d 0 and 2. Mice were scored and weighed daily until the end of the experiment on d 32. Shown are the mean cumulative and maximal scores (\pm SEM). Asterisk indicates the control group.

1.5% of the CD4⁺ repertoire. 2D2-FIG and 2D2-FIG *Csf2*^{-/-} mice were pretreated with PC61 or Y13 mAb and were sensitized for EAE induction (Fig. 3G and H). Regardless of mAb pretreatment, all 4 groups had severe acute EAE. However, control (Y13-treated) 2D2-FIG *Csf2*^{-/-} mice exhibited a partial recovery by d 20, whereas the other 3 groups maintained a severe chronic course of EAE. These data reveal a second model, whereby active immunization of 2D2-FIG *Csf2*^{-/-} mice drove EAE despite a global deficiency in GM-CSF. The caveat was that the presence of GM-CSF (i.e., 2D2-FIG mice treated with Y13) or depletion of CD25⁺ T_{regs} in the absence of GM-CSF (i.e., 2D2-FIG *Csf2*^{-/-} mice treated with PC61) reversed the spontaneous recovery noted in Y13-pretreated 2D2-FIG *Csf2*^{-/-} mice. This model reinforces the concept that EAE susceptibility is contingent upon a GM-CSF-dependent balance among conventional and regulatory subsets.

To assess the efficiency of PC61-mediated depletion of CD25⁺ FOXP3⁺ T_{regs}, FIG *Csf2*^{-/-} and control FIG mice were treated with 250 µg PC61 or Y13 on d -4 and -2, and PBMCs were analyzed on d 0 (Fig. 3I–O). These analyses revealed that *Csf2*^{-/-} mice had profound perturbations of leukocyte subsets, including elevated percentages of Ly6G⁺ granulocytes (Fig. 3I), depressed percentages of CD19⁺ B cells (Fig. 3J), and increased percentages of CD3⁺ T cells (Fig. 3K) relative to the total leukocyte/WBC pool. *Csf2*^{-/-} mice also had depressed CD8⁺ percentages (Fig. 3L) and elevated CD4⁺ percentages (Fig. 3M) in the CD3⁺ T cell compartment. Notably, pretreatment with PC61 did not affect the percentages of these leukocyte and T cell subsets. FIG *Csf2*^{-/-} mice had decreased percentages of FOXP3⁺ T cells in the CD4⁺ compartment compared with FIG mice (Fig. 3N). In that FOXP3⁺ T cells were comprised of both CD25⁺ and CD25⁻ subsets, PC61 treatment was found to reduce total percentages of circulating FOXP3⁺ T cells as a result of the elimination of CD25⁺ FOXP3⁺ T_{regs} but not CD25⁻ FOXP3⁺ T cells (Fig. 3O). That is, in PC61-treated mice, surviving FOXP3⁺ T_{regs} did not express CD25, as measured by MFI. Thus, the ability of PC61 to enable EAE in

Csf2^{-/-} mice was correlated with the specific elimination of the CD25⁺ FOXP3⁺ subset rather than the CD25⁻ FOXP3⁺ subset.

In regard to Fig. 3C–F, anti-CD4 or anti-CD8 mAb treatment was shown to eliminate specifically the CD4⁺ and CD8⁺ subsets, respectively (Fig. 3P and Q). As an expected consequence of subset-specific deletion, anti-CD4 treatment augmented percentages of CD8⁺ T cells, and anti-CD8 treatment augmented percentages of CD4⁺ T cells in the CD3⁺ pool. Anti-CD4 treatment also completely eliminated T_{regs} (Fig. 3R), as FOXP3⁺ T cells were exclusively CD4⁺ T cells (data not shown). PC61 treatment substantially depleted FOXP3⁺ T_{regs}, and surviving T_{regs} had baseline (negative) expression of CD25 (Fig. 3S). Quality control experiments in reference to Fig. 3G and H showed that CD8⁺ T cells (0.47% ± 0.21%, 0.77 ± 0.21) and FOXP3⁺ T cells (0.53% ± 0.15%, 0.87 ± 0.25) each comprised <1% of the “2D2-FIG *Csf2*^{-/-}” and 2D2-FIG T cell repertoires, respectively (Fig. 3T–V). These data verified that the 2D2-FIG was an EAE model naturally deficient in both CD8⁺ T cells and FOXP3⁺ T_{regs}.

A passive model of EAE was also used to assess whether PC61 enabled the induction of GM-CSF-deficient encephalitogenic T cells in *Csf2*^{-/-} mice (Table 4 and Fig. 4). Donor *Csf2*^{-/-} mice and donor C57BL/6 mice were or were not treated with 250 µg PC61 on d -5 and -3 and then were immunized with MOG35–55 in CFA on d 0. Draining lymph nodes and splenocytes from each of the 4 donor groups were pooled on d 11 and were cultured for 3 d with 1 µM MOG35–55 and 10 ng/ml IL-23. Activated, nonfractionated donor T cells (10⁷/recipient) were then adoptively transferred into recipients. *Csf2*^{-/-} T cells were injected into *Csf2*^{-/-} recipients, and C57BL/6 T cells were injected into C57BL/6 recipients. On d 7 after adoptive transfer, each recipient group was or was not injected with 250 µg PC61 (8 groups, *n* = 4/group). Two conclusions were evident. First, PC61 treatment of *Csf2*^{-/-} donors enabled the differentiation of encephalitogenic T cells and the adoptive transfer of paralytic EAE into *Csf2*^{-/-} recipients. PC61 pretreatment of *Csf2*^{-/-} donors resulted in

TABLE 4. The anti-CD25 PC61 mAb enables the adoptive transfer of EAE in *Csf2*^{-/-} mice

Strain	Donors	Recipients	Incidence	Mean cumulative score	Median cumulative score	Mean maximal score	Median maximal score	Mean maximal weight loss	Mean average weight loss
(a) <i>Csf2</i> ^{-/-}	PC61	PC61	4 of 4	109.7 ± 7.4	108.5	4.0 ± 0.0	4.0	20.4%	13.7%
(b) <i>Csf2</i> ^{-/-}	PC61	Saline	4 of 4	53.8 ± 19.1	60.3	3.0 ± 0.7	3.5	17.9%	12.4%
(c) <i>Csf2</i> ^{-/-}	Saline	PC61	0 of 4	0.0 ± 0.0	0.0	0.0 ± 0.0	0.0	0.0%	-3.0%
(d) <i>Csf2</i> ^{-/-}	Saline	Saline	0 of 4	0.0 ± 0.0	0.0	0.0 ± 0.0	0.0	0.0%	-0.8%
(e) C57BL/6	PC61	PC61	4 of 4	119.8 ± 1.8	120.3	4.0 ± 0.0	4.0	26.9%	21.2%
(f) C57BL/6	PC61	Saline	4 of 4	67.6 ± 4.6	71.0	4.0 ± 0.0	4.0	28.1%	17.7%
(g) C57BL/6	Saline	PC61	4 of 4	123.5 ± 2.1	123.0	4.0 ± 0.0	4.0	22.5%	18.4%
(h) C57BL/6	Saline	Saline	4 of 4	91.9 ± 12.8	81.0	4.0 ± 0.0	4.0	27.3%	18.0%
(c) and (d) vs. (a), (e), (g), and (h)			<i>P</i> = 0.0286	<i>P</i> ≤ 0.002		<i>P</i> ≤ 0.001		<i>P</i> ≤ 0.001	<i>P</i> ≤ 0.017

These data are portrayed in Fig. 4. Donor *Csf2*^{-/-} and control C57BL/6 mice were or were not treated with 250 µg PC61 on d -5 and -3 and were immunized with 200 µg MOG35–55 in CFA on d 0. On d 11, draining lymph nodes and spleen were pooled within each of the 4 donor groups. These cells were cultured for 3 d with 1 µM MOG35–55 and 10 ng/ml IL-23. Activated donor T cells were then adoptively transferred into recipients (10⁷ cells/recipient). *Csf2*^{-/-} T cells were injected into *Csf2*^{-/-} recipients, and C57BL/6 T cells were injected into C57BL/6 recipients. On d 7, each recipient group was or was not injected with 250 µg PC61. Shown are the means and the SEM for cumulative and maximal EAE scores. Differences in EAE and weight-loss values were assessed by nonparametric and parametric ANOVA, respectively. Differences in disease incidence were assessed pairwise by a Fisher's exact test.

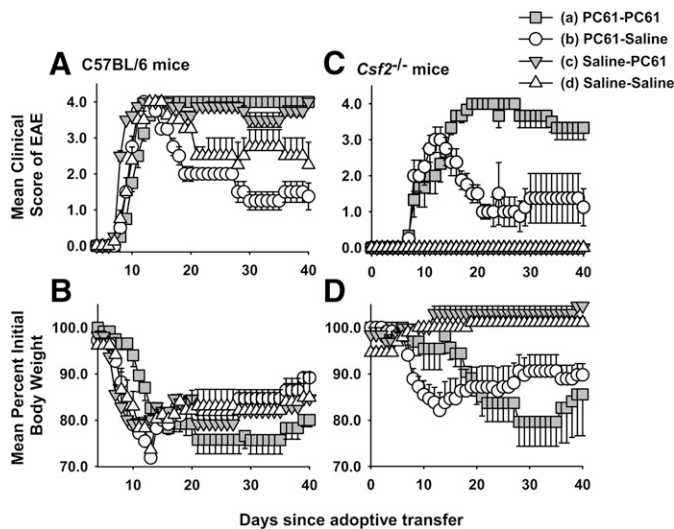


Figure 4. The PC61 anti-CD25 mAb enable the passive induction of EAE in *Csf2*^{-/-} mice. Shown are time courses of data portrayed in Table 4. PC61-PC61, both donors and recipients were treated with PC61; PC61-Saline, donors but not recipients were treated with PC61; Saline-PC61, recipients but not donors were treated with PC61; Saline-Saline, neither donors nor recipients were treated with PC61. Shown are the means and the SEM for the EAE score (A and C) and weight loss (B and D) time courses of C57BL/6 (A and B) and *Csf2*^{-/-} (C and D) mice. (C) Nonparametric ANOVA; (a) vs. (c) and (d), $P < 0.004$ from d 8 to 40; (b) vs. (d), $P < 0.001$ from d 8 to 17 and $P < 0.05$ from d 18 to 40; and (b) vs. (a), $P < 0.05$ from d 17 to 29. (D) Parametric ANOVA; (a) vs. (c) and (d), $P < 0.020$ from d 27 to 38; (b) vs. (d), $P < 0.010$ from days 9 to 18; (b) vs. (c), $P < 0.02$ from d 9 to 20 and $P < 0.05$ from d 21 to 26; and (b) vs. (a), $P < 0.32$ from d 13 to 15.

cumulative and maximal disease scores of 53.8 and 3.0, respectively, in recipients, whereas control *Csf2*^{-/-} donor T cells did not transfer EAE to recipients [(b) vs. (d); Table 4]. The main conclusion was that PC61 enabled encephalitogenic sensitization of *Csf2*^{-/-} donor T cells. Second, PC61 treatment of both donors and recipients enabled chronic EAE in recipient *Csf2*^{-/-} mice, whereas pretreatment of donors alone resulted in an initial bout of severe EAE in recipients, followed by a partial recovery [(b) vs. (a); Table 4 and Fig. 4C]. These data provided evidence that CD4⁺ CD25⁺ T_{regs} prevented the differentiation of encephalitogenic T cells in *Csf2*^{-/-} donor mice and blunted the action of established pathogenic T cells in *Csf2*^{-/-} recipient mice. Differences in the time courses of EAE were paralleled by differences in maximal and average weight loss (Fig. 4B and D). All 4 groups of C57BL/6 recipients exhibited severe paralytic EAE (Fig. 4A). Nonetheless, PC61 treatment of recipient C57BL/6 mice prevented partial recovery and maintained EAE scores near a maximum of 4.0 (full hindlimb paralysis of both legs) during the entire 40 d observation period. These data provided evidence that CD4⁺ CD25⁺ T_{regs} may also modify passively induced EAE in wt recipients.

Csf2^{-/-} mice exhibited alterations in the relative distribution of lymphocyte subsets

As noted previously in Figs. 1 and 3, *Csf2*^{-/-} mice had profoundly altered percentages of leukocyte and lymphoid

subsets. In CD4⁺ and CD8⁺ subsets, quiescent FSC^{low} T cells from *Csf2*^{-/-} peripheral blood had low levels of CD44 surface expression compared with WT controls (Fig. 5A and B). Experiments comparing *Csf2*^{-/-} with WT splenocytes showed essentially equivalent differences among leukocyte subset percentages and CD44 expression as those noted in PBMCs (data not shown). FSC^{low} CD4⁺ T cells constituted the majority of CD4⁺ T cells in *Csf2*^{-/-} blood (72%) and a relative minority of CD4⁺ T cells (37%) in C57BL/6 blood (Fig. 5A). These representative percentages are portrayed as bar graphs ($n = 6$) in Fig. 5E. Not only were FSC^{low} CD4⁺ T cells predominant in *Csf2*^{-/-} blood, but also, these *Csf2*^{-/-} CD4⁺ T cells expressed substantially less CD44 than the equivalent FSC^{low} CD4⁺ subset in C57BL/6 blood (Fig. 5A and F). In contrast, enlarged FSC^{high} *Csf2*^{-/-} CD4⁺ T cells had CD44 levels that were commensurate with WT controls (Fig. 5A and F). Overall, these findings revealed a significant difference in quiescent memory between the 2 mouse strains. Similar findings were noted for the CD8⁺ T cell subset. In both *Csf2*^{-/-} and C57BL/6 blood, most CD8⁺ T cells had a small FSC^{low} phenotype, and FSC^{low} CD8⁺ T cells from *Csf2*^{-/-} blood expressed substantially lower levels of CD44 than FSC^{low} CD8⁺ T cells from C57BL/6 blood (Fig. 5B, E, and F).

In contrast to FSC^{low} T cells, *Csf2*^{-/-} granulocytes had CD44 levels similar to that of WT controls (Fig. 5C and G). *Csf2*^{-/-} PBMCs had significantly higher percentages of Ly-6G⁺ granulocytes compared with C57BL/6 PBMCs, although the frequencies of CD11b⁺ blood monocytes were similar between the 2 strains (data not shown). Indeed, the average percentage of Ly-6G⁺ granulocytes ($n = 6$) was 3.8-fold greater than in C57BL/6 mice. As noted in splenocytes (not shown), CD19⁺ B cells were substantially less frequent in *Csf2*^{-/-} PBMCs (excluding granulocytes; 23%) compared with WT PBMCs (65%; Fig. 5D). All B cells expressed CD44, and *Csf2*^{-/-} B cells had CD44 levels similar to that of C57BL/6 B cells (Fig. 5D and G). As shown in Fig. 5D, both *Csf2*^{-/-} and C57BL/6 CD19⁺ B cells had similar levels of CD44, whereas the non-B cell fraction (mostly T cells) exhibited profound differences in the percentages of CD44^{low} vs. CD44^{high} subsets (Fig. 5G and H).

Absolute leukocyte counts assessed by use of reference beads revealed no significant differences in the absolute numbers of viable PBMCs and CD45⁺ leukocytes in the blood of *Csf2*^{-/-} and C57BL/6 mice. Absolute leukocyte counts in PBMCs revealed that the *Csf2*^{-/-} mutation was associated with profound alterations in major leukocyte subsets, including CD4⁺CD3⁺ T cells, CD8⁺CD3⁺ T cells, B cells, and granulocytes. *Csf2*^{-/-} PBMCs contained a 3.4-fold increase in numbers of CD11b⁺Ly-6G⁺ granulocytes, a 1.9-fold increase in numbers of CD3⁺ T cells, a 1.5-fold increase in CD3⁺ CD8⁺ T cells, and a 2.4-fold increase in CD3⁺ CD4⁺ T cells. Conversely, C57BL/6 PBMCs contained a 2.8-fold increase in CD19⁺ B cells ($n = 6$). Overall, the altered frequencies of lymphoid cell types were consistent between the blood and the spleen, such that the blood was a reliable indicator of the cell-type percentages in the spleen. The increased numbers of CD4⁺ and CD8⁺ T cells in *Csf2*^{-/-} mice were largely attributed to increased cellularity of the naïve CD44^{low} T cell compartments. Increased absolute numbers but decreased percentages of CD8⁺ T cells (e.g., Figs. 1 and 3) simply reflected the predominant accumulation of naïve CD4⁺ T cells.

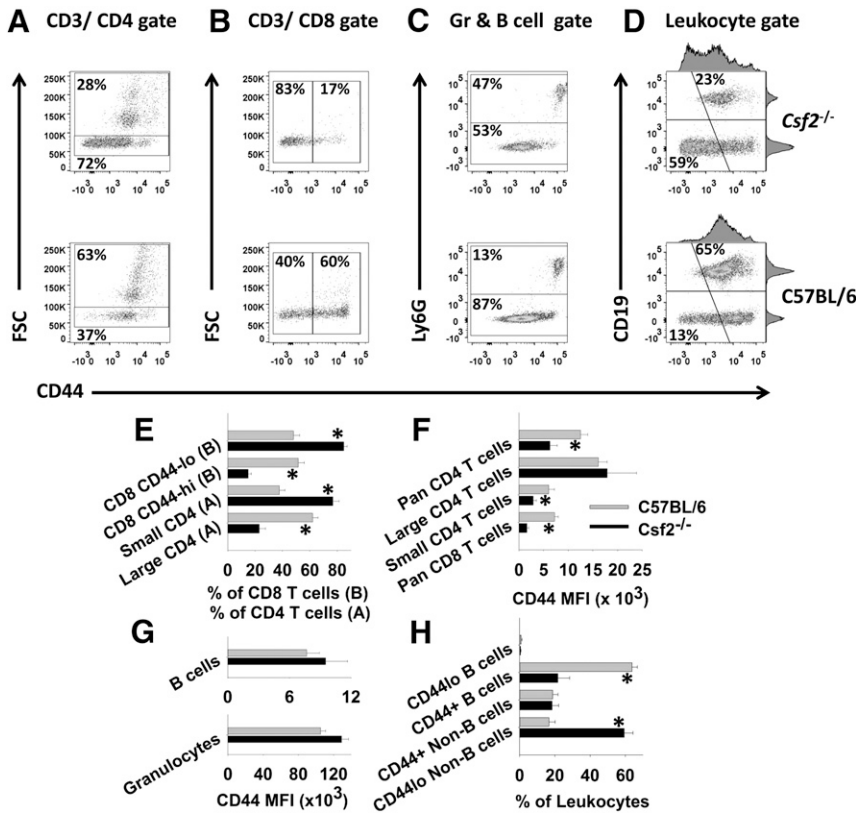


Figure 5. *Csf2*^{-/-} mice show altered T cell expression of CD44. PBMCs from 6 *Csf2*^{-/-} and 6 C57BL/6 were stained with fluorochrome-conjugated antibodies against CD45, CD3, CD4, CD8, CD44, Ly-6G, or CD19. Dot plots (upper) show data from a representative mouse from each group, and the associated bar graphs (lower) show the means and SD of each group (*n* = 6 mice). Gated populations of CD3⁺CD4⁺ T cells (A, E, and F) and CD3⁺CD8⁺ T cells (B, E, and F) were analyzed for FSC and CD44 expression. (C and G) A granulocyte (Gr)–B cell gate was used to analyze CD44 levels on the respective subsets. (D and H) A leukocyte gate (excluding granulocytes) was used to analyze CD44 expression on B cells and non-B cells (mostly T cells). The bar graphs show the mean percentage of the designated subsets (E and H) or the MFI for CD44 expression (F and G) together with the SD (**P* < 0.001). These data are representative of 4 independent experiments.

Given that GM-CSF deficiency caused profound perturbations of major T cell subsets, an important question was how the GM-CSF deficiency-affected percentages of CD4⁺ CD25⁺ FOXP3⁺ T_{regs}. FIG *Csf2*^{-/-} and FIG mice were used in these experiments. Like *Csf2*^{-/-} PBMC and splenocytes, FIG *Csf2*^{-/-} PBMCs had elevated frequencies of total CD3⁺ T cells and a predominance of CD4⁺ T cells (Fig. 6A). Shown are the percentages of CD3⁺ T cells in reference to total leukocytes (excluding granulocytes) and the percentages of CD4⁺ T cells in the CD3⁺ T cell pool (Fig. 6A). As shown for *Csf2*^{-/-} mice (Fig. 5), elevated percentages of CD3⁺ T cells in FIG *Csf2*^{-/-} PBMC were associated with increased frequencies of small, quiescent CD4⁺ and CD8⁺ subsets (Fig. 6B). The percentages of FSC^{low} CD4⁺ and FSC^{low} CD8⁺ T cells are shown in reference to the total pools of CD4⁺ and CD8⁺ T cells, respectively. Essentially, all GFP⁺ (FOXP3⁺) T cells were CD4⁺ (data not shown). Frequencies of CD4⁺ CD25⁺ FOXP3⁺ T cells were reduced in FIG *Csf2*^{-/-} PBMCs when total CD3⁺ T cells were used as the baseline (Fig. 6C). These reductions were modest but statistically significant (*P* < 0.001). Larger reductions were noted when total CD4⁺ T cells or FSC^{high} CD4⁺ T cells were used as the denominator of the ratio. Thus, T_{reg} percentages in FIG *Csf2*^{-/-} mice were modestly decreased when normalized to CD3⁺ T cells and more substantially decreased when normalized to CD4⁺ T cells or FSC^{high} CD4⁺ T cells. These data indicate that the GM-CSF deficiency is not associated with elevated T_{reg} percentages (Fig. 6C) or T_{reg} numbers (data not shown).

The large accumulation of naïve CD44^{low} T cells in *Csf2*^{-/-} mice suggested that GM-CSF deficiency conferred deficient immunogenic sensitization to environmental antigens. Likewise,

GM-CSF deficiency, at least in part, may confer EAE resistance by undermining encephalitogenic sensitization in MOG/CFA-challenged mice, as previously noted in Fig. 4. Deficient T_{conv} responses balanced by a functionally intact T_{reg} repertoire would accommodate the main observation of this study—that PC61 liberates encephalitogenic responses in *Csf2*^{-/-} mice. To test this hypothesis, *Csf2*^{-/-} and C57BL/6 mice were pretreated with PC61 or Y13 mAb on d -4 and -2, were challenged on d 0 with MOG35–55 in CFA, and were given Ptx on d 0 and 2. On d 12, these sensitized C57BL/6 mice and PC61-pretreated *Csf2*^{-/-} mice began exhibiting clinical signs of EAE (score of 3.0 and 2.0, respectively), whereas Y13-pretreated *Csf2*^{-/-} mice remained resistant to EAE. Lymphoid cells were isolated from draining nodes, labeled with CellTrace Violet (Thermo Fisher Scientific), and cultured with 1 μM MOG35–55 for 4 d. The results showed that CD4⁺ T cells from the draining lymph nodes of PC61-pretreated *Csf2*^{-/-} mice, but not those from Y13-pretreated *Csf2*^{-/-} mice, exhibited robust MOG-specific proliferation (Fig. 7A). Similar MOG-specific proliferative responses were noted in the CD8⁺ T and B cell compartments (Fig. 7B and C). The latter observation presumably reflected bystander proliferation as a result of cytokine production by MOG-stimulated CD4⁺ T cells. Parallel cultures of C57BL/6 showed high levels of background proliferation. This observation may reflect more efficient transport of MOG from the MOG/CFA emulsion into the draining lymphatics, as in vitro proliferation was not dependent on exogenously added MOG. We also noted that CD8⁺ T cell proliferation from Y13-pretreated C57BL/6 mice was substantially higher than that from PC61-treated C57BL/6 mice. This

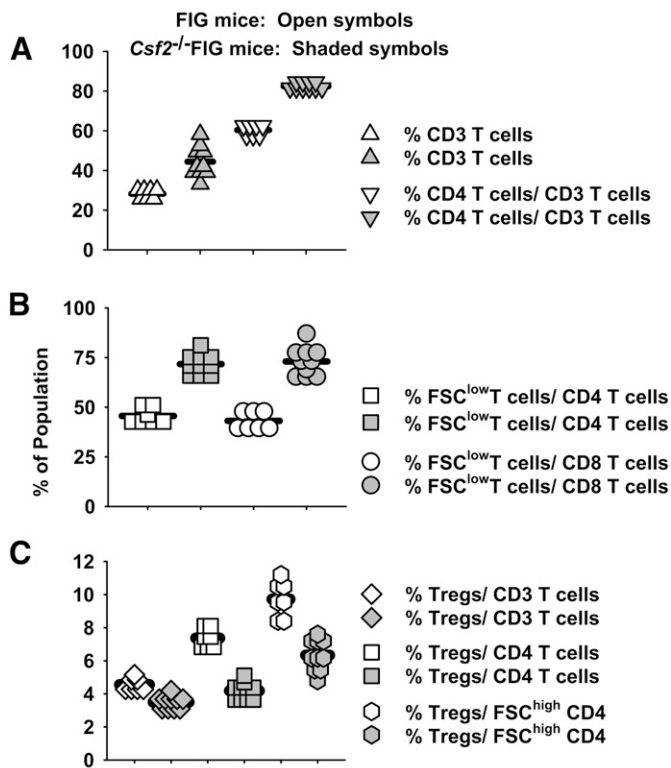


Figure 6. Percentages of CD4⁺ CD25⁺ FOXP3⁺ T_{regs} in Csf2^{-/-} exhibit modest reductions in frequency relative to the pool of total CD3⁺ T cell. PBMCs were obtained from 7 Csf2^{-/-} FIG mice and 10 FIG mice. (A) Shown are the percentages of CD3⁺ T cells among total leukocytes (excluding granulocytes) and the percentage of CD4⁺ T cells among the total CD3⁺ T cell pool. (B) Shown are the percentages of FSC^{low} CD4⁺ T cells among the total CD4⁺ T cell pool and the percentages of FSC^{low} CD8⁺ T cells among the total CD8⁺ T cell pool. (C) Shown are the percentages of CD4⁺ CD25⁺ FOXP3⁺ T_{regs} among the CD3⁺ T cell pool, the CD3⁺ CD4⁺ T cell pool, and the FSC^{high} CD3⁺ CD4⁺ T cell pool. *t* Tests revealed significant differences for all 7 pairwise comparisons (A–C; *P* < 0.001). These data are representative of 3 independent experiments.

result may reflect PC61-mediated depletion of CD25⁺ CD8⁺ precursors in vivo. Based on the analysis of PC61 vs. Y-13-treated Csf2^{-/-} mice, these data indicate that GM-CSF is needed for MOG-specific CD4⁺ T cells to overcome T_{reg} barriers during encephalitogenic sensitization in the lymphatics draining a MOG/CFA inoculation.

DISCUSSION

Severe chronic EAE can be elicited in Csf2^{-/-} mice

This study was based on the observation that pretreatment with the PC61 anti-CD25 mAb enabled the expression of severe EAE in the otherwise resistant Csf2^{-/-} strain. Although Csf2^{-/-} mice are profoundly resistant to EAE, previous studies provided evidence that resistance could be bypassed by intracranial inoculation of LPS or TLR9 agonists simultaneously with the adoptive transfer of MBP-specific Csf2^{-/-} T cells into WT recipients [19]. Although recipients were

GM-CSF replete, EAE effector T cells represented the key source of GM-CSF, as MBP–TCR transgenic T cells transferred EAE into WT and Csf2^{-/-} recipients, whereas MBP–TCR Csf2^{-/-} T cells lacked the ability to transfer EAE into WT recipients. Presumably, direct stimulation of TLRs in the CNS compensated for the lack of GM-CSF production by MBP-specific Csf2^{-/-} T cells in the CNS, thereby resulting in the activation of microglia, CNS infiltration of peripheral myeloid cells, enhanced effector T cell infiltration, and the reconstitution of EAE. MBP–TCR transgenic mice were used to bypass any role that GM-CSF may play during clonal expansion and in vivo sensitization. However, as recipients were GM-CSF replete, and many cell types produce GM-CSF, these studies could not exclude the possibility that TLR-stimulated GM-CSF in the host contributed to EAE in this model [19].

Data shown in Figs. 1–4 complement and extend these studies by showing that severe chronic EAE can be readily induced in an unambiguous GM-CSF-deficient model, including active induction of EAE in Csf2^{-/-} mice and adoptive transfer of Csf2^{-/-} T cells into Csf2^{-/-} recipients. The mechanism of EAE resistance in Csf2^{-/-} mice was abrogated by treatment of Csf2^{-/-} mice with the PC61 anti-CD25 mAb that eliminated CD4⁺ CD25⁺ FOXP3⁺ T_{regs}. PC61-treated Csf2^{-/-} mice exhibited disease time courses and severities that were essentially the same as those in WT mice. As PC61 did not affect CD25⁺ FOXP3⁺ T_{regs}, the implication was that the normal effector CD25⁺ FOXP3⁺ T_{reg} subset represented a major mechanism of disease resistance in Csf2^{-/-} mice. We considered 2 overlapping possibilities to explain the role of CD25⁺ T_{regs} in GM-CSF-deficient mice. First, T_{conv} responses may be impaired, whereas T_{reg} barriers may be essentially normal and functionally intact. Second, T_{conv} responses may be essentially normal, whereas T_{reg} responses may be expanded or hyperfunctional.

The first hypothesis (i.e., impaired T_{conv} repertoire) was directly supported by the observation that both CD4 and CD8 T cell repertoires were dominated by quiescent, naïve CD44^{low} T cells (Fig. 5). The large accumulation of CD44^{low} naïve T cells in Csf2^{-/-} mice most likely reflected a requirement for GM-CSF in normal sensitization to environmental antigens. This hypothesis was also directly supported by the observation that Csf2^{-/-} mice had a profound defect in encephalitogenic sensitization (Fig. 4). Initial studies showing that Csf2^{-/-} mice were profoundly resistant to EAE also revealed that MOG35–55/CFA-sensitized mice exhibited depressed MOG-specific splenocyte proliferation and reduced production of IL-2, IL-6, and IFN-γ [6]. GM-CSF was also needed for induction of CD103⁺ DCs in peripheral lymphoid tissues and the consequent differentiation of naïve, myelin-reactive T cells into clonally expanded IFN-γ effector T cells [33]. These observations showed that GM-CSF has an important role in sensitization of encephalitogenic responses. This finding was confirmed by data in Fig. 7. MOG/CFA-immunized Csf2^{-/-} mice lacked ex vivo reactivity to MOG, whereas PC61 pretreatment of Csf2^{-/-} mice enabled vigorous anti-MOG CD4⁺ T cell responses ex vivo, together with recruitment of CD8⁺ and B cell responses. We also noted that the draining lymph nodes of MOG35–55/CFA-sensitized Csf2^{-/-} mice were at least 2 times smaller, on average, than the nodes of WT mice

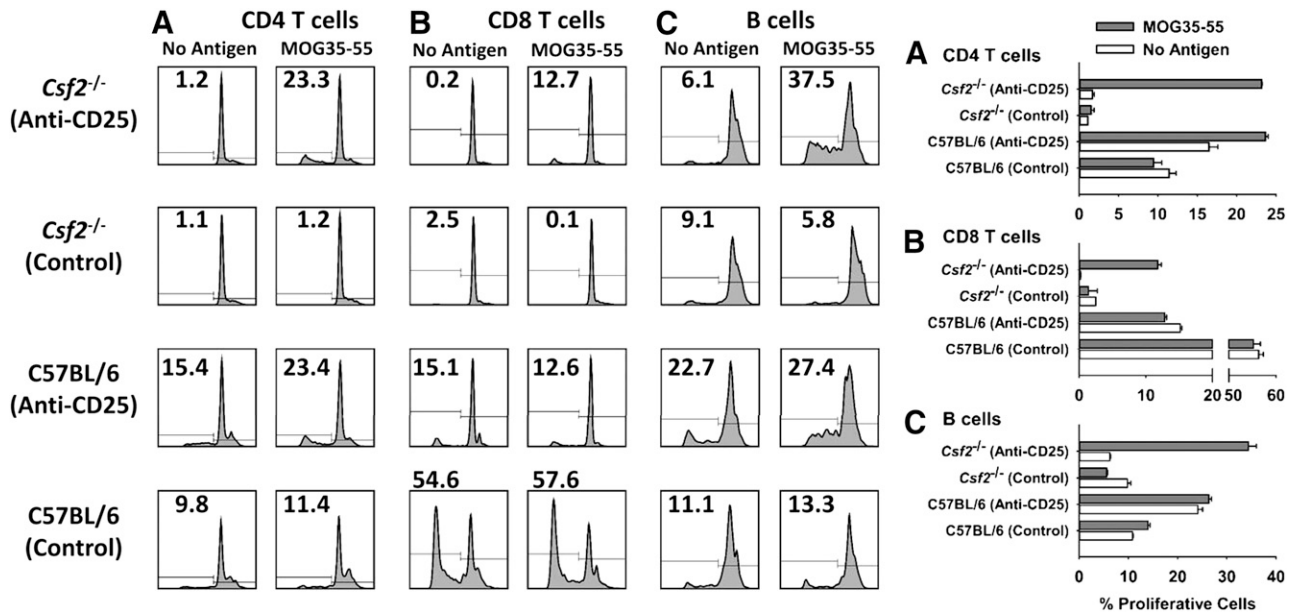


Figure 7. MOG-specific sensitization is deficient in *Csf2*^{-/-} mice. *Csf2*^{-/-} and C57BL/6 mice were pretreated with 250 μ g PC61 or Y13 mAb on d -4 and -2 and were challenged on d 0 with MOG35-55 in CFA. Ptx was given on d 0 and 2. On d 12, lymphoid cells were isolated from draining nodes; labeled with CellTrace Violet; cultured in triplicate, with or without 1 μ M MOG35-55 for 4 d; and analyzed for expression of CD45, CD3, CD4, CD19, and MHC class II. B Cells were gated as the CD19⁺, MHC class II⁺ population. CellTrace Violet dye dilution was used as a measure of proliferation. (A–C) PC61-pretreated *Csf2*^{-/-} cultures \pm 1 μ M MOG35-55 ($P < 0.001$). Y13-pretreated *Csf2*^{-/-} cultures \pm 1 μ M MOG35-55 (not significant). These data are representative of 3 replicate experiments.

(data not shown). Overall, these observations indicate that *Csf2*^{-/-} mice had a profound defect in antigenic priming.

The second hypothesis (i.e., T_{reg} hyper-reactivity) was less consistent with our experimental observations, particularly in that the activated/effector subset of CD25⁺ FOXP3⁺ T_{regs} in *Csf2*^{-/-} mice did not exhibit evidence of expansion in blood or secondary lymphoid organs (Figs. 1, 3, and 6). If the T_{reg} repertoire were expanded or hyperfunctional, one would expect exaggerated tolerogenic responses. However, immunization of *Csf2*^{-/-} mice with MOG did not increase numbers, percentages, or activation phenotypes of T_{regs} compared with WT mice, and tolerogenic vaccination of *Csf2*^{-/-} mice did not elicit more T_{regs} than observed in WT mice (data not shown). Rather, *Csf2*^{-/-} mice exhibited deficient immunogenic responsiveness, not hyper-reactive tolerance, as the unresponsive state was readily reversed by administration of exogenous GM-CSF [6]. Likewise, EAE in WT mice was blocked by anti-GM-CSF therapy, but withdrawal of the antibody resulted in the rapid return of severe clinical symptoms [6, 14]. If GM-CSF deficiency conferred the hyperinduction of tolerance, then the unresponsive state would persist beyond the simple reconstitution of GM-CSF. In the absence of GM-CSF, weakened T_{conv} responses apparently lacked the activation energy to overcome the normal barriers imposed by CD25⁺ T_{regs}. However, upon mAb-mediated depletion of CD25⁺ T_{regs}, encephalitogenic sensitization was unimpeded by T_{regs} and culminated in severe chronic EAE. Overall, this study supports the concept that EAE resistance of *Csf2*^{-/-} mice was a result of a functional imbalance of functionally deficient effector responses and functional

CD25⁺ T_{regs}. These observations favor the view that the PC61 sensitivity of *Csf2*^{-/-} mice is not a result of gross alteration of the T_{reg} repertoire but rather, reflected subjugation of a compromised T_{conv} repertoire.

An anti-CD25 mAb represented the tool used to deplete FOXP3⁺ T_{regs} in this study. FOXP3⁺ T_{regs} exist as CD25⁺ and CD25⁻ subsets, and the PC61 mAb specifically depleted CD25⁺ FOXP3⁺ T_{regs} but not CD25⁻ FOXP3⁺ T cells (Fig. 3). CD25⁺ FOXP3⁺ T_{regs} represent activated, functional T_{regs}, whereas CD25⁻ FOXP3⁺ T cells are quasi-stable T_{regs} that represent transitional phases between T_{conv} and functional T_{regs} [34–36]. Although PC61 is typically thought to work by depletion of FOXP3⁺ T_{regs}, this study cannot exclude the possibility that PC61 enabled EAE in *Csf2*^{-/-} mice by depletion of alternative CD25⁺ regulatory cells aside from the FOXP3 lineage. Additional research focusing on more direct manipulation of the FOXP3⁺ T cell subset will be needed to address this possibility.

GM-CSF is required for pathogenic invasion of the CNS

Several lines of evidence implicated T cell-mediated production of GM-CSF as a critical proinflammatory mediator in the effector phase of EAE. For example, adoptive transfer of IFN- γ ^{-/-} T cells into IL-17RA^{-/-} recipients was completely inhibited by treatment with an anti-GM-CSF antibody [15]. Additional adoptive transfer studies also implicated T cell-mediated production of GM-CSF as a key event in the effector phase of CNS pathogenesis [16]. IL-17^{-/-}, IFN- γ ^{-/-}, or dual-deficient polyclonal T cells or IL-17^{-/-} 2D2 T cells had potent EAE transfer activity, but *Csf2*^{-/-} polyclonal T cells or polarized Th1/Th17 *Csf2*^{-/-} 2D2 T cells

lacked EAE-inductive activity. GM-CSF-deficient and -replete Th1 and Th17 T cells from the transgenic MBP(Ac1–11) clonotype exhibited similar dependency of GM-CSF production for adoptive EAE [14]. *Csf2*^{-/-} effector cells exhibited early CNS infiltration but did not sustain CNS inflammation as a result of defects in the recruitment of peripheral myeloid CD45^{high}, CD11b myeloid cells [6, 14]. Conditional gene targeting revealed that GM-CSF responsiveness of peripheral CCR2⁺ Ly6C^{high} monocytes was required for EAE [37]. Whether GM-CSF is important for surmounting T_{reg} barriers at the effector phase remains an important question. PC61 treatment of recipients in the *Csf2*^{-/-} adoptive transfer system prevented partial recovery from EAE (Fig. 4). Likewise, PC61 pretreatment of actively immunized 2D2-FIG *Csf2*^{-/-} mice also prevented spontaneous recovery (Fig. 3). These data indicate that GM-CSF has a continuing role to counter T_{reg} responses during the effector/recovery phase of chronic EAE.

Paradoxically, GM-CSF can be used to induce tolerance in EAE

One might surmise that a major action of GM-CSF is to enable T_{conv} to overcome T_{reg} barriers during sensitization and effector phases of EAE. However, the regulatory action of GM-CSF is complex. A substantial literature linked the presence (not the absence) of GM-CSF to the induction of "regulatory" DCs and T_{regs} in several models of autoimmune disease [38–48]. Likewise, GM-CSF–neuroantigen fusion proteins had potent tolerogenic and therapeutic action in rat and mouse models of EAE [49–51]. GM-CSF–neuroantigen fusion proteins mediated a dominant tolerogenic action even when introduced into the strongly proinflammatory environment of the CFA lymphatic drainage [52]. Thus, GM-CSF apparently facilitates dominance of T_{conv} or T_{reg} responses based on adaptive cues in the local environment.

GM-CSF is required for the normal balance of leukocyte subsets, including granulocytes, B cells, and naïve vs. effector T cells

Given that GM-CSF has direct action on myeloid rather than lymphoid cells as a result of the presence of the respective receptor on myeloid APCs but not on T and B cells, it was notable that GM-CSF deficiency had profound effects on numbers and percentages of lymphoid subsets. Most importantly, *Csf2*^{-/-} mice had elevated percentages of CD3⁺ T cells and increased percentages of CD44^{null-low} naïve T cells in CD4⁺ and CD8⁺ T cell compartments. The likelihood is that *Csf2*^{-/-} DCs and T cells exhibit an altered antigen-driven development as a result of intertwined mechanisms, in which the lack of GM-CSF production by antigen-stimulated T cells causes deficient DC maturation. The lack of myeloid DC differentiation may, in turn, engender deficient presentation of ubiquitous environmental antigens that, in turn, impair the differentiation of naïve T cells into memory cells. This bottleneck in T cell development may account for the accumulation of naïve, quiescent CD44^{null/low} T cells and the deficiency in CD44^{high} memory T cells in *Csf2*^{-/-} mice.

The main myeloid perturbation noted in this study was an ~3-fold increase in the percentages of granulocytes in *Csf2*^{-/-}

PBMCs. The impact of GM-CSF upon the granulocytic lineage may be multifold. Granulocytes express the GM-CSFR heterodimer and directly respond to GM-CSF by induction of effector activities. However, GM-CSF-stimulated production of reactive oxygen intermediates may shorten the granulocyte lifespan. GM-CSF production by tissue-resident myeloid APCs and effector-memory T cells may induce chemokines that promote migration of granulocytes from the blood into peripheral tissues. Thus, the absence of GM-CSF in *Csf2*^{-/-} mice may thereby lengthen the granulocyte lifespan and/or persistence of granulocytes in the circulation and thereby, increase detection of granulocytes in blood. Another possibility is that the balance of GM-CSF and G-CSF may influence the proportional differentiation of monocytic and granulocytic lineages in the bone marrow. The absence of GM-CSF in *Csf2*^{-/-} mice may result in unbalanced G-CSF-induced differentiation of myeloid precursors into the granulocytic lineage. However, percentages of CD11b⁺ monocytes were not significantly different in *Csf2*^{-/-} and WT PBMCs (data not shown). Many other nonexclusive possibilities also may account for the accentuated frequencies of granulocytes in *Csf2*^{-/-} mice.

Conclusion

The presence of maximal EAE in the complete absence of GM-CSF revealed that GM-CSF is not an obligate effector molecule in all forms of EAE. This study instead supports the alternative explanation that the EAE resistance of *Csf2*^{-/-} mice, at least in part, was a result of a functional imbalance of T_{regs} and effector T cells. These observations reveal a link between deficient T cell differentiation, a functional T_{reg}/T_{conv} imbalance, and EAE resistance in *Csf2*^{-/-} mice.

AUTHORSHIP

D.G. performed the majority of the experiments. A.D.C. and D.S.W. facilitated the experimentation, including the histological analysis and mAb purification/quality control. M.D.M. played a major role in the conception and design of the study, generation of antibody supernatants, compilation of the data, and writing of the manuscript. All authors were important intellectual contributors to this study.

ACKNOWLEDGMENTS

This study was supported by the National Institute of Neurological Disorders and Stroke, U.S. National Institutes of Health (Grants R15-NS075830 and R01-NS072150, to M.D.M.) and the Harriet and John Wooten Laboratory for Alzheimer's and Neurodegenerative Disease Research (to M.D.M.) and by a research grant from AlzNC, Alzheimer's North Carolina.

DISCLOSURES

The authors have no financial or commercial conflicts of interest in regard to this work.

REFERENCES

1. Robinson, A. P., Harp, C. T., Noronha, A., Miller, S. D. (2014) The experimental autoimmune encephalomyelitis (EAE) model of MS: utility for understanding disease pathophysiology and treatment. *Handb. Clin. Neurol.* **122**, 173–189.
2. Ben-Nun, A., Kaushansky, N., Kawakami, N., Krishnamoorthy, G., Berer, K., Liblau, R., Hohlfeld, R., Wekerle, H. (2014) From classic to spontaneous and humanized models of multiple sclerosis: impact on understanding pathogenesis and drug development. *J. Autoimmun.* **54**, 33–50.
3. Simmons, S. B., Pierson, E. R., Lee, S. Y., Goverman, J. M. (2013) Modeling the heterogeneity of multiple sclerosis in animals. *Trends Immunol.* **34**, 410–422.
4. Rangachari, M., Kuchroo, V. K. (2013) Using EAE to better understand principles of immune function and autoimmune pathology. *J. Autoimmun.* **45**, 31–39.
5. Kuerten, S., Lehmann, P. V. (2011) The immune pathogenesis of experimental autoimmune encephalomyelitis: lessons learned for multiple sclerosis? *J. Interferon Cytokine Res.* **31**, 907–916.
6. McQualter, J. L., Darwiche, R., Ewing, C., Onuki, M., Kay, T. W., Hamilton, J. A., Reid, H. H., Bernard, C. C. (2001) Granulocyte macrophage colony-stimulating factor: a new putative therapeutic target in multiple sclerosis. *J. Exp. Med.* **194**, 873–882.
7. Mendel, I., Katz, A., Kozak, N., Ben-Nun, A., Revel, M. (1998) Interleukin-6 functions in autoimmune encephalomyelitis: a study in gene-targeted mice. *Eur. J. Immunol.* **28**, 1727–1737.
8. Samoilova, E. B., Horton, J. L., Hilliard, B., Liu, T. S., Chen, Y. (1998) IL-6-deficient mice are resistant to experimental autoimmune encephalomyelitis: roles of IL-6 in the activation and differentiation of autoreactive T cells. *J. Immunol.* **161**, 6480–6486.
9. Becher, B., Segal, B. M. (2011) T(H)17 cytokines in autoimmune neuroinflammation. *Curr. Opin. Immunol.* **23**, 707–712.
10. Liu, X., Lee, Y. S., Yu, C. R., Egwuagu, C. E. (2008) Loss of STAT3 in CD4⁺ T cells prevents development of experimental autoimmune diseases. *J. Immunol.* **180**, 6070–6076.
11. Chitnis, T., Najafian, N., Benou, C., Salama, A. D., Grusby, M. J., Sayegh, M. H., Khoury, S. J. (2001) Effect of targeted disruption of STAT4 and STAT6 on the induction of experimental autoimmune encephalomyelitis. *J. Clin. Invest.* **108**, 739–747.
12. Behrens, F., Tak, P. P., Ostergaard, M., Stoilov, R., Wiland, P., Huizinga, T. W., Berenfs, V. Y., Vladava, S., Rech, J., Rubbert-Roth, A., Korkosz, M., Rekalov, D., Zupanets, I. A., Ejbjerg, B. J., Geiseler, J., Fresenius, J., Korolkiewicz, R. P., Schottelius, A. J., Burkhardt, H. (2015) MOR103, a human monoclonal antibody to granulocyte-macrophage colony-stimulating factor, in the treatment of patients with moderate rheumatoid arthritis: results of a phase Ib/Ia randomised, double-blind, placebo-controlled, dose-escalation trial. *Ann. Rheum. Dis.* **74**, 1058–1064.
13. Deiß, A., Brecht, I., Haarmann, A., Buttmann, M. (2013) Treating multiple sclerosis with monoclonal antibodies: a 2013 update. *Expert Rev. Neurother.* **13**, 313–335.
14. El-Behi, M., Ciric, B., Dai, H., Yan, Y., Cullimore, M., Safavi, F., Zhang, G. X., Dittel, B. N., Rostami, A. (2011) The encephalitogenicity of T(H)17 cells is dependent on IL-1 and IL-23-induced production of the cytokine GM-CSF. *Nat. Immunol.* **12**, 568–575.
15. Kroenke, M. A., Chensue, S. W., Segal, B. M. (2010) EAE mediated by a non-IFN- γ /non-IL-17 pathway. *Eur. J. Immunol.* **40**, 2340–2348.
16. Codarri, L., Gyölvézi, G., Tosevski, V., Hesske, L., Fontana, A., Magnenat, L., Suter, T., Becher, B. (2011) ROR γ t drives production of the cytokine GM-CSF in helper T cells, which is essential for the effector phase of autoimmune neuroinflammation. *Nat. Immunol.* **12**, 560–567.
17. Flügel, A., Berkowicz, T., Ritter, T., Labeur, M., Jenne, D. E., Li, Z., Ellwart, J. W., Willem, M., Lassmann, H., Wekerle, H. (2001) Migratory activity and functional changes of green fluorescent effector cells before and during experimental autoimmune encephalomyelitis. *Immunity* **14**, 547–560.
18. Kawakami, N., Lassmann, S., Li, Z., Odoardi, F., Ritter, T., Ziemssen, T., Klinkert, W. E., Ellwart, J. W., Bradl, M., Krivacic, K., Lassmann, H., Ransohoff, R. M., Volk, H. D., Wekerle, H., Linington, C., Flügel, A. (2004) The activation status of neuroantigen-specific T cells in the target organ determines the clinical outcome of autoimmune encephalomyelitis. *J. Exp. Med.* **199**, 185–197.
19. Ponomarev, E. D., Shriver, L. P., Maresz, K., Pedras-Vasconcelos, J., Verthelyi, D., Dittel, B. N. (2007) GM-CSF production by autoreactive T cells is required for the activation of microglial cells and the onset of experimental autoimmune encephalomyelitis. *J. Immunol.* **178**, 39–48.
20. Kroenke, M. A., Carlson, T. J., Andjelkovic, A. V., Segal, B. M. (2008) IL-12- and IL-23-modulated T cells induce distinct types of EAE based on histology, CNS chemokine profile, and response to cytokine inhibition. *J. Exp. Med.* **205**, 1535–1541.
21. McGeachy, M. J. (2011) GM-CSF: the secret weapon in the T(H)17 arsenal. *Nat. Immunol.* **12**, 521–522.
22. Dranoff, G., Crawford, A. D., Sadelain, M., Ream, B., Rashid, A., Bronson, R. T., Dickersin, G. R., Bachurski, C. J., Mark, E. L., Whitsett, J. A., Mulligan, R. C. (1994) Involvement of granulocyte-macrophage colony-stimulating factor in pulmonary homeostasis. *Science* **264**, 713–716.
23. Lublin, F. D., Knobler, R. L., Kalman, B., Goldhaber, M., Marini, J., Perrault, M., D'Imperio, C., Joseph, J., Alkan, S. S., Korngold, R. (1993) Monoclonal anti-gamma interferon antibodies enhance experimental allergic encephalomyelitis. *Autoimmunity* **16**, 267–274.
24. Duong, T. T., Finkelman, F. D., Singh, B., Strejan, G. H. (1994) Effect of anti-interferon-gamma monoclonal antibody treatment on the development of experimental allergic encephalomyelitis in resistant mouse strains. *J. Neuroimmunol.* **53**, 101–107.
25. Krakowski, M., Owens, T. (1996) Interferon-gamma confers resistance to experimental allergic encephalomyelitis. *Eur. J. Immunol.* **26**, 1641–1646.
26. Willenborg, D. O., Fordham, S., Bernard, C. C., Cowden, W. B., Ramshaw, I. A. (1996) IFN-gamma plays a critical down-regulatory role in the induction and effector phase of myelin oligodendrocyte glycoprotein-induced autoimmune encephalomyelitis. *J. Immunol.* **157**, 3223–3227.
27. Chu, C. Q., Wittmer, S., Dalton, D. K. (2000) Failure to suppress the expansion of the activated CD4 T cell population in interferon gamma-deficient mice leads to exacerbation of experimental autoimmune encephalomyelitis. *J. Exp. Med.* **192**, 123–128.
28. Sasaki, K., Bean, A., Shah, S., Schutten, E., Huseby, P. G., Peters, B., Shen, Z., Vanguri, V., Liggitt, D., Huseby, E. S. (2014) Relapsing-remitting central nervous system autoimmunity mediated by GFAP-specific CD8⁺ T cells. *J. Immunol.* **192**, 3029–3042.
29. Ji, Q., Goverman, J. (2007) Experimental autoimmune encephalomyelitis mediated by CD8⁺ T cells. *Ann. N. Y. Acad. Sci.* **1103**, 157–166.
30. Ford, M. L., Evavold, B. D. (2005) Specificity, magnitude, and kinetics of MOG-specific CD8⁺ T cell responses during experimental autoimmune encephalomyelitis. *Eur. J. Immunol.* **35**, 76–85.
31. Sun, D., Whitaker, J. N., Huang, Z., Liu, D., Coleclough, C., Wekerle, H., Raine, C. S. (2001) Myelin antigen-specific CD8⁺ T cells are encephalitogenic and produce severe disease in C57BL/6 mice. *J. Immunol.* **166**, 7579–7587.
32. Huseby, E. S., Liggitt, D., Brabb, T., Schnabel, B., Ohlén, C., Goverman, J. (2001) A pathogenic role for myelin-specific CD8⁺ T cells in a model for multiple sclerosis. *J. Exp. Med.* **194**, 669–676.
33. King, I. L., Kroenke, M. A., Segal, B. M. (2010) GM-CSF-dependent, CD103⁺ dermal dendritic cells play a critical role in Th effector cell differentiation after subcutaneous immunization. *J. Exp. Med.* **207**, 953–961.
34. Huynh, A., DuPage, M., Priyadharshini, B., Sage, P. T., Quiros, J., Borges, C. M., Townamchai, N., Gerriets, V. A., Rathmell, J. C., Sharpe, A. H., Bluestone, J. A., Turka, L. A. (2015) Control of PI(3) kinase in Treg cells maintains homeostasis and lineage stability. *Nat. Immunol.* **16**, 188–196.
35. Komatsu, N., Okamoto, K., Sawa, S., Nakashima, T., Oh-hora, M., Kodama, T., Tanaka, S., Bluestone, J. A., Takayanagi, H. (2014) Pathogenic conversion of Foxp3⁺ T cells into TH17 cells in autoimmune arthritis. *Nat. Med.* **20**, 62–68.
36. Ohkura, N., Hamaguchi, M., Morikawa, H., Sugimura, K., Tanaka, A., Ito, Y., Osaki, M., Tanaka, Y., Yamashita, R., Nakano, N., Huehn, J., Fehling, H. J., Sparwasser, T., Nakai, K., Sakaguchi, S. (2012) T cell receptor stimulation-induced epigenetic changes and Foxp3 expression are independent and complementary events required for Treg cell development. *Immunity* **37**, 785–799.
37. Croxford, A. L., Lanzinger, M., Hartmann, F. J., Schreiner, B., Mair, F., Pelczar, P., Clausen, B. E., Jung, S., Greter, M., Becher, B. (2015) The cytokine GM-CSF drives the inflammatory signature of CCR2⁺ monocytes and licenses autoimmunity. *Immunity* **43**, 502–514.
38. Gopisetty, A., Bhattacharya, P., Haddad, C., Bruno, J. C., Jr., Vasu, C., Miele, L., Prabhakar, B. S. (2013) OX40L/Jagged1 cosignaling by GM-CSF-induced bone marrow-derived dendritic cells is required for the expansion of functional regulatory T cells. *J. Immunol.* **190**, 5516–5525.
39. Sheng, J. R., Muthusamy, T., Prabhakar, B. S., Meriggioli, M. N. (2011) GM-CSF-induced regulatory T cells selectively inhibit anti-acetylcholine receptor-specific immune responses in experimental myasthenia gravis. *J. Neuroimmunol.* **240–241**, 65–73.
40. Bhattacharya, P., Gopisetty, A., Ganesh, B. B., Sheng, J. R., Prabhakar, B. S. (2011) GM-CSF-induced, bone-marrow-derived dendritic cells can expand natural Tregs and induce adaptive Tregs by different mechanisms. *J. Leukoc. Biol.* **89**, 235–249.
41. Ganesh, B. B., Cheatem, D. M., Sheng, J. R., Vasu, C., Prabhakar, B. S. (2009) GM-CSF-induced CD11c⁺CD8 α ⁺ dendritic cells facilitate Foxp3⁺ and IL-10⁺ regulatory T cell expansion resulting in suppression of autoimmune thyroiditis. *Int. Immunol.* **21**, 269–282.

42. Cheatem, D., Ganesh, B. B., Gangi, E., Vasu, C., Prabhakar, B. S. (2009) Modulation of dendritic cells using granulocyte-macrophage colony-stimulating factor (GM-CSF) delays type 1 diabetes by enhancing CD4+CD25+ regulatory T cell function. *Clin. Immunol.* **131**, 260–270.
43. Sheng, J. R., Li, L. C., Ganesh, B. B., Prabhakar, B. S., Meriggioli, M. N. (2008) Regulatory T cells induced by GM-CSF suppress ongoing experimental myasthenia gravis. *Clin. Immunol.* **128**, 172–180.
44. Gaudreau, S., Guindi, C., Ménard, M., Besin, G., Dupuis, G., Amrani, A. (2007) Granulocyte-macrophage colony-stimulating factor prevents diabetes development in NOD mice by inducing tolerogenic dendritic cells that sustain the suppressive function of CD4+CD25+ regulatory T cells. *J. Immunol.* **179**, 3638–3647.
45. Sheng, J. R., Li, L., Ganesh, B. B., Vasu, C., Prabhakar, B. S., Meriggioli, M. N. (2006) Suppression of experimental autoimmune myasthenia gravis by granulocyte-macrophage colony-stimulating factor is associated with an expansion of FoxP3+ regulatory T cells. *J. Immunol.* **177**, 5296–5306.
46. Gangi, E., Vasu, C., Cheatem, D., Prabhakar, B. S. (2005) IL-10-producing CD4+CD25+ regulatory T cells play a critical role in granulocyte-macrophage colony-stimulating factor-induced suppression of experimental autoimmune thyroiditis. *J. Immunol.* **174**, 7006–7013.
47. Vasu, C., Dogan, R. N., Holterman, M. J., Prabhakar, B. S. (2003) Selective induction of dendritic cells using granulocyte macrophage-colony stimulating factor, but not fms-like tyrosine kinase receptor 3-ligand, activates thyroglobulin-specific CD4+/CD25+ T cells and suppresses experimental autoimmune thyroiditis. *J. Immunol.* **170**, 5511–5522.
48. Gaudreau, S., Guindi, C., Ménard, M., Benabdallah, A., Dupuis, G., Amrani, A. (2010) GM-CSF induces bone marrow precursors of NOD mice to skew into tolerogenic dendritic cells that protect against diabetes. *Cell. Immunol.* **265**, 31–36.
49. Mannie, M. D., Blanchfield, J. L., Islam, S. M., Abbott, D. J. (2012) Cytokine-neuroantigen fusion proteins as a new class of tolerogenic, therapeutic vaccines for treatment of inflammatory demyelinating disease in rodent models of multiple sclerosis. *Front. Immunol.* **3**, 255.
50. Abbott, D. J., Blanchfield, J. L., Martinson, D. A., Russell, S. C., Taslim, N., Curtis, A. D., Mannie, M. D. (2011) Neuroantigen-specific, tolerogenic vaccines: GM-CSF is a fusion partner that facilitates tolerance rather than immunity to dominant self-epitopes of myelin in murine models of experimental autoimmune encephalomyelitis (EAE). *BMC Immunol.* **12**, 72.
51. Blanchfield, J. L., Mannie, M. D. (2010) A GMCSF-neuroantigen fusion protein is a potent tolerogen in experimental autoimmune encephalomyelitis (EAE) that is associated with efficient targeting of neuroantigen to APC. *J. Leukoc. Biol.* **87**, 509–521.
52. Islam, S. M., Curtis, A. D., Taslim, N., Wilkinson, D. S., Mannie, M. D. (2014) GM-CSF-neuroantigen fusion proteins reverse experimental autoimmune encephalomyelitis and mediate tolerogenic activity in adjuvant-primed environments: association with inflammation-dependent, inhibitory antigen presentation. *J. Immunol.* **193**, 2317–2329.

KEY WORDS:

multiple sclerosis · FOXP3⁺ T cells · tolerance · neuroimmunology